

PAPER • OPEN ACCESS

## Defects in the long-range $O(N)$ model

To cite this article: Lorenzo Bianchi *et al* 2025 *J. Phys. A: Math. Theor.* **58** 335401

View the [article online](#) for updates and enhancements.

### You may also like

- [Magic angle \(in\)stability and mobility edges in disordered Chern insulators](#)  
Simon Becker, Izak Oltman and Martin Vogel
- [Unfolding the six-dimensional tensor multiplet](#)  
Carlo Iazeolla, Per Sundell and Brenno Carlini Vallilo
- [Commentary and Notes on the Original Derivations of the Scharifker-Hills Model](#)  
Yunkai Sun and Giovanni Zangari

# Defects in the long-range $O(N)$ model

Lorenzo Bianchi<sup>1,2,\*</sup> , Leonardo S Cardinale<sup>3</sup>   
and Elia de Sabbata<sup>2,4</sup> 

<sup>1</sup> Dipartimento di Fisica, Università di Torino and INFN—Sezione di Torino, Via P. Giuria 1, 10125 Torino, Italy

<sup>2</sup> I.N.F.N.—sezione di Torino, Via P. Giuria 1, I-10125 Torino, Italy

<sup>3</sup> Département de Physique, Ecole Normale Supérieure—PSL, 24 Rue Lhomond, 75005 Paris, France

<sup>4</sup> Dipartimento di Scienze e Innovazione Tecnologica, Università del Piemonte Orientale, Via T. Michel 11, 15121 Alessandria, Italy

E-mail: [lorenzo.bianchi@unito.it](mailto:lorenzo.bianchi@unito.it), [leonardo.cardinale@ens.psl.eu](mailto:leonardo.cardinale@ens.psl.eu) and [eliadesabbata@gmail.com](mailto:eliadesabbata@gmail.com)

Received 8 April 2025; revised 16 July 2025

Accepted for publication 4 August 2025

Published 13 August 2025



CrossMark

## Abstract

We initiate the study of extended excitations in the long-range  $O(N)$  model. We focus on line and surface defects and we discuss the challenges of a naive generalization of the simplest defects in the short-range model. To face these challenges we propose three alternative realizations of defects in the long-range model. The first consists in introducing an additional parameter in the perturbative RG flow or, equivalently, treating the non-locality of the model as a perturbation of the local four-dimensional theory. The second is based on the introduction of non-local defect degrees of freedom coupled to the bulk and it provides some non-trivial defect CFTs also in the case of a free bulk, i.e. for generalized free field theory. The third approach is based on a semiclassical construction of line defects. After finding a non-trivial classical field configuration we consider the fluctuation Lagrangian to obtain quantum corrections for the defect theory.

Keywords: defects, long-range Ising model, conformal bootstrap, conformal field theories

\* Author to whom any correspondence should be addressed.



Original Content from this work may be used under the terms of the [Creative Commons Attribution 4.0 licence](https://creativecommons.org/licenses/by/4.0/). Any further distribution of this work must maintain attribution to the author(s) and the title of the work, journal citation and DOI.

## Contents

1. Introduction and discussion	2
2. The model and its defects	5
2.1. The long-range $O(N)$ model	5
2.2. Existence and classification of some non-trivial defects	8
2.2.1. Local defects	9
2.2.2. Non-local defects	9
2.2.3. Semiclassical defects	10
3. Non-local defects	11
3.1. $(a, b) = (1, 2)$	14
3.2. $(a, b) = (2, 1)$	15
3.3. $(a, b) = (2, 2n)$	16
3.4. $a$ odd or $b$ odd	17
3.5. The line defect for general $b$	19
3.6. Summary	19
4. Defects in the long-range $O(N)$ model close to four dimensions	20
4.1. Localized magnetic field	22
4.2. Surface defect	24
5. Semiclassical construction of defects	26
5.1. A warm-up example	26
5.2. The long-range $O(N)$ model	28
5.2.1. Semiclassics	28
5.2.2. Quantum corrections	29
Data availability statement	31
Acknowledgments	31
Appendix A. Diagrams for the defect coupling renormalization	32
Appendix B. Useful integrals	33
Appendix C. Diagrams for the $g$ -function close to four dimensions	33
C.1. Useful integrals for the computation of $g$ -functions	34
Appendix D. Integrating out $\psi$	35
D.1. $b = 1$ theory	35
D.2. $b = 2$ theory	36
References	38

## 1. Introduction and discussion

Recent developments in our understanding of quantum field theories (QFTs) have profoundly transformed how we conceptualize and approach these theories. Symmetries and general consistency conditions, such as unitarity and locality, have turned out to be much more constraining than we had previously thought, and finding the best ways to impose these constraints has spurred a major line of research. These considerations have led to several important results in various areas, such as scattering amplitudes, cosmology and conformal field theory. The application to the latter, commonly known as the conformal bootstrap, has yielded some unprecedented predictions for the critical exponents of statistical models (see [1] for a review), paving the way for a fruitful exchange with the condensed matter community.

While the assumption of locality is very natural in the context of QFTs, we know that realistic statistical models, such as spin lattices, might have long-range interactions, leading to

a non-local description in the continuum limit. The long-range Ising (LRI) model, for instance, is a generalization of the short-range Ising (SRI) model where the interaction is weighted by a power of the distance between the nodes. The continuum description of this theory is a non-local QFT, which displays an interesting phase diagram depending on the value of the exponent in the power law [2–5]. In particular, for dimension  $2 < d < 4$ , there is an interesting region of the phase diagram where the fixed point is actually an interacting non-local conformal field theory. This phase space has been known since the seventies [2–5] and its shape has been supported both by RG flow analyzes [6, 7] and Monte Carlo simulations [8–12]. More recently, the authors of [13] provided a formal proof of the conformal invariance of the model, while in [14, 15] a novel UV description was proposed to study the LRI model at the crossover with the SRI. Perturbative results for critical exponents in various long-range  $O(N)$  models have been obtained in [16–18]. Bootstrap methods have been applied to the LRI model in [19, 20], while large- $N$  analysis for the long-range  $O(N)$  model have been explored in [21–23]. Fermionic generalizations have been considered as well [24]. Finally, recent work has investigated the structure of long-range perturbation theory and the mechanisms for conformality loss near the short-range crossover [25, 26].

In this paper, we initiate the study of the LRI model in the presence of defects. Defects are important observables in QFTs and statistical mechanics [27]. In particular, a wide range of defects has been studied in the short-range critical  $O(N)$  model from a condensed matter perspective, including impurities [28–32] and boundaries [33–36]. Moreover, defects in the short-range critical  $O(N)$  model have also been extensively studied using a field-theoretical framework. In particular, numerical and analytic bootstrap techniques have been applied to boundaries [37–39] and line defects [40–44]. Furthermore, the  $\varepsilon$ -expansion and the large- $N$  expansion have been used to extract information about line defects [45–52], surface defects [48, 49, 52–56], and boundaries [52, 57, 58], as well as to explore more exotic constructions such as intersecting or transdimensional defects [59, 60]. Finally, boundaries in the long-range  $O(N)$  model have been considered in [61]. Here we take the first steps towards the generalization of these constructions to the case of the long-range  $O(N)$  model. There are different methods to approach the long-range fixed point in the literature, including large  $N$ , large charge and  $\varepsilon$  expansions. In the latter case, one of the attractive features of long-range models is that the presence of an additional parameter  $\sigma$  for the strength of the interaction, which decays as  $|x|^{d+\sigma}$ , allows us to perform an  $\varepsilon$ -expansion at fixed dimension  $d$ , where  $\varepsilon = 2\sigma - d$  parametrizes the distance from the crossover  $\sigma = \frac{d}{2}$  with the Gaussian theory. The goal of this work is to introduce defects in the UV theory and look for the existence of non-trivial defect CFTs in the IR through an  $\varepsilon$ -expansion analysis of the RG flow.

### *Summary of the results*

We start our analysis from line and surface defects, which are realized, in the short-range model, by integrating classically marginal operators on the defect. The simplest examples are the localized magnetic field, where a single scalar field is integrated along a line, and surface defects involving the integration of a quadratic combination of fields. The general idea of these constructions is to analyze the behavior of the defect coupling in the  $\varepsilon$ -expansion and look for non-trivial perturbative fixed points. A naive generalization of these constructions turns out to work only close to four dimensions, where the integrated operators are classically marginal. As we mentioned, one of the important features of the long-range models is the possibility to work at fixed  $d$  expanding around the crossover. Therefore, some non-trivial generalization is required to study defects in this regime. This is one of the goals of the present work. A more

technical overview of our approach is given in section 2.2. Here we shortly summarize our findings:

- *Non-local defects* (section 3). We construct a whole new class of defects by introducing non-local scalar degrees of freedom on the defect and coupling them with the bulk scalars. We study some general restrictions on the form of such couplings and then we analyze the existence of some non-trivial fixed point in the simplest cases. One important consequence of this approach is that we will be able to construct non-trivial defects in generalized free field (GFF) theory.
- *Defects close to four dimensions* (section 4). We generalize the construction of line and surface defects for the SRI model using the ordinary  $\varepsilon$ -expansion, but introducing an additional parameter that allows us to explore the long-range IR fixed points. This is equivalent to interpreting the non-locality of the model as a perturbation of the local four-dimensional theory.
- *Semiclassical defects* (section 5). To describe the localized magnetic field away from four dimensions, we develop a semiclassical approach. We look for non-trivial classical solutions for the field, whose form is consistent with the requirements of defect conformal field theories (in particular this solution is singular on the defect profile). Perturbation theory around this saddle provides a complicated fluctuation Lagrangian, which can be used to compute various observables in the defect CFT.

As will be explained in more detail in the next sections, each of the above approaches has its own strengths and weaknesses. For instance, the main advantage of the *non-local defects* discussed in section 3 is that they can be studied through perturbative techniques while working directly in  $d = 3$  dimensions. This comes at the cost of introducing new degrees of freedom on the defect. As a consequence, a potential lattice description of these defects becomes more complicated. On the other hand, the approach used in section 4 allows one to study a model with a simpler lattice description. However, the drawback is that one must work in  $d = 4 - \varepsilon$  dimensions, and some resummation technique is required to extract information about the more physical three-dimensional theory, even when the bulk theory is perturbatively close to the GFF theory. Finally, the semiclassical approach outlined in section 5 applies to the same defects as the latter, and in principle can be used directly in  $d = 3$ . However, in practice, computations are considerably more complicated, and we were only able to perform them to a limited extent.

### Outlook

This paper is the first attempt to introduce impurities in the long-range  $O(N)$  model and, as such, it opens up a variety of new interesting future directions. The first comment is that we used only one of the techniques that are available in these models, i.e. the  $\varepsilon$ -expansion. It would be interesting to analyze our constructions with other methods, such as large  $N$  or large charge expansions.

Non-perturbative approaches, such as Monte Carlo simulations or numerical bootstrap would also be extremely useful. For the former, it would be interesting to understand how to realize on the lattice the non-local defects we construct here. For the latter, the most natural question is whether one could find interesting constraints in the space of defects, even starting from the case of GFF theories, where we found a new class of interesting defects. In this respect, an active research direction focuses on the study of conformal defects in free theories [62–66] and our work goes in the direction of understanding what happens if one relaxes the condition of locality.

Pushing our perturbative analysis to higher orders is an obvious and natural development and it would be interesting to combine this with the analytic bootstrap approach, along the lines of what has been done for the short-range model [40–43]. The most natural observables for this analysis would be the defect four-point function and the bulk two-point function, where the crossing equations might help to recover the perturbative results by symmetry considerations, without resorting to Feynman diagrams.

The part of the LRI phase space that we explore in this paper is formed by the region around  $d=4$  and that around the crossover  $\sigma = d/2$  with the Gaussian theory. Nevertheless, there is also another interesting region one could explore that is the ‘upper’ crossover, drawing the boundary between the LRI and SRI phases. A novel perspective on how to approach this crossover has been put forward in [15] and it would be interesting to insert defects into that picture.

Finally, let us mention that the long-range perturbation theory has been recently used as a complementary way to extract information about the short-range model [25]. This has the advantage that one can work at fixed space dimension, but, since perturbation theory is performed around the Gaussian crossover, obtaining information about the opposite crossover requires a resummation of the perturbative series. Still, it is an interesting approach and it would be nice to exploit it also in the case of defects. For instance, one natural question regards the fate of the non-local defects when we approach the SRI crossover. Do they produce new non-trivial defects in the short-range model?

## 2. The model and its defects

### 2.1. The long-range $O(N)$ model

This work focuses primarily on the LRI model and its  $O(N)$  vector extension in dimensions  $2 < d < 4$ . The LRI model can be defined on a spin lattice through the following Hamiltonian:

$$H = -J \sum_{i \neq j} \frac{s_i s_j}{|i - j|^{d+\sigma}}, \quad (2.1)$$

where we take  $J > 0$  to stick to the ferromagnetic case. This model undergoes a second-order phase transition at a certain critical temperature  $T = T_c$ . Following the standard Landau-Ginzburg approach, at  $T = T_c$ , it is possible to replace the discrete model with the following action of an interacting real massless scalar field

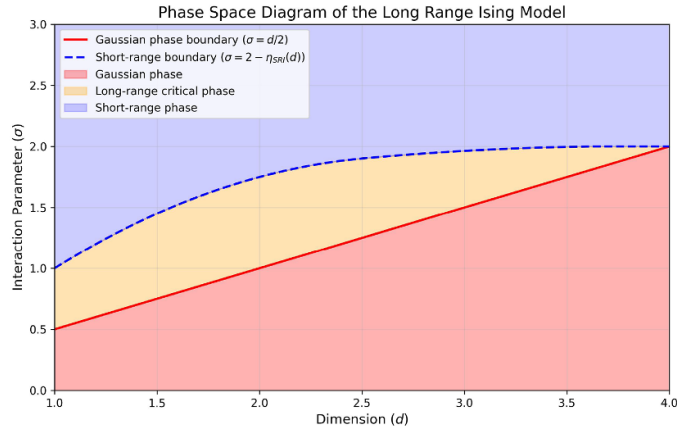
$$S = \frac{\mathcal{N}_\sigma}{2} \int d^d x d^d y \frac{\phi(x) \phi(y)}{|x - y|^{d+\sigma}} + \frac{\lambda_0}{4!} \int d^d x \phi(x)^4, \quad (2.2)$$

with a normalization constant  $\mathcal{N}_\sigma$  fixed such that in momentum space the kinetic part of the action reads  $\frac{1}{2} \int \frac{d^d p}{(2\pi)^d} \phi(-p) |p|^\sigma \phi(p)$ . Such a normalization is given by

$$\mathcal{N}_\sigma = \frac{2^\sigma \Gamma(\frac{d+\sigma}{2})}{\pi^{\frac{d}{2}} \Gamma(-\frac{\sigma}{2})}. \quad (2.3)$$

Henceforth, we will refer to this continuum action as the LRI model. The generalization to the long-range  $O(N)$  model is straightforward. One can promote  $\phi$  to an  $O(N)$  vector field,  $\phi^a$ , where  $a = 1, \dots, N$ , and contract the indices in the natural way

$$S = \frac{\mathcal{N}_\sigma}{2} \int d^d x d^d y \frac{\phi_a(x) \phi_a(y)}{|x - y|^{d+\sigma}} + \frac{\lambda_0}{4!} \int d^d x (\phi_a(x) \phi_a(x))^2. \quad (2.4)$$



**Figure 1.** Phase space diagram for the long-range Ising model as a function of the dimension  $d$  and the parameter  $\sigma$ . The diagram shows the Gaussian phase ( $\sigma \leq d/2$ ), the long-range critical phase ( $d/2 < \sigma < 2 - \eta_{\text{SRI}}(d)$ ), and the short-range phase ( $\sigma \geq 2 - \eta_{\text{SRI}}(d)$ ).

The case  $N = 1$  reduces to the LRI model (2.2).

The actions (2.2) and (2.4) are clearly non-local. More precisely, an action is *local* if it involves a single integral of the fields and their derivatives up to a finite order. In contrast, actions that depend on an infinite number of field derivatives or involve more than one integral are usually referred to as *non-local* (see [67] for a modern treatment of this subject). The non-local kinetic term can also be rewritten using of the fractional Laplacian  $\mathcal{L}_\sigma = (-\partial^2)^{\sigma/2}$ , where  $\sigma$  is a real number. This operator acts on plane waves as  $\mathcal{L}_\sigma e^{ipx} = |p|^\sigma e^{ipx}$ , and in position space it is given by

$$\mathcal{L}_\sigma \phi(x) = \mathcal{N}_\sigma \int d^d y \frac{\phi(y)}{|x-y|^{d+\sigma}}. \tag{2.5}$$

Using this notation, the kinetic term becomes

$$S_{\text{kin}} = \frac{1}{2} \int d^d x \phi(x) \mathcal{L}_\sigma \phi(x), \tag{2.6}$$

which leads to the following classical scaling dimension

$$\Delta_\phi = \frac{d-\sigma}{2}. \tag{2.7}$$

When  $\sigma = 2$  the fractional Laplacian reduces to the usual Laplacian and the theory becomes the more familiar quartic theory that describes the SRI model.

The LRI has a rich phase space structure that depends on the value of  $\sigma$  [13, 15, 68]. This is illustrated in figure 1:

- For  $\sigma < d/2$ , the quartic interaction is irrelevant, and the theory becomes free in the infrared (IR). In particular, it is a GFF theory with  $\Delta_\phi$  given in (2.7).
- For  $\sigma > \sigma_* = d - 2\Delta_\phi^{\text{SRI}}$ , where  $\Delta_\phi^{\text{SRI}}$  is the conformal dimension of  $\phi$  in the SRI model, the critical theory reduces to the SRI model.

- For  $d/2 < \sigma < \sigma_*$ , the critical theory is non-trivial and non-Gaussian. Indeed, the quartic interaction is relevant and drives the theory towards an IR fixed point, known as the LRI fixed point (see figure 1).

Similar statements apply to the  $O(N)$  generalization of the LRI.

There is another way to get to the action in equation (2.2), where one interprets the LRI as a defect of dimension  $d$  embedded in a bulk space of (generically non-integer) dimension  $d - \sigma + 2$ . Specifically, if one considers a local massless field  $\Phi(x, y)$  with action

$$S = \int d^d x d^{2-\sigma} y \left[ (\partial_x \Phi)^2 + (\partial_y \Phi)^2 \right] + \int_{y=0} d^d x \Phi^4, \quad (2.8)$$

then integrating out the bulk field  $\Phi(x, y \neq 0)$  leads to a theory for  $\phi(x) = \Phi(x, 0)$ , which is identical to the LRI theory. This method is sometimes referred to as the Caffarelli–Silvestre trick [69]. In fact, this perspective is particularly useful for proving that the LRI exhibits enhanced conformal symmetry at the IR fixed point [13].

The free propagator of the long-range  $O(N)$  model can be easily derived

$$G_{ab}(x) = \frac{2^{d-\sigma} \Gamma\left(\frac{d-\sigma}{2}\right)}{(4\pi)^{\frac{d}{2}} \Gamma\left(\frac{\sigma}{2}\right)} \frac{\delta_{ab}}{|x|^{d-\sigma}} = \frac{\mathcal{N}_\phi^2 \delta_{ab}}{|x|^{2\Delta_\phi}}. \quad (2.9)$$

To study the LRI fixed point perturbatively, the standard approach is to perform an  $\varepsilon$ -expansion near the crossover  $\sigma = d/2$ , as shown in figure 1. However, it is also useful to introduce a second type of expansion close to the corner  $d = 4$ . For clarity and to set up the notation, we present both expansions here.

- Setting  $\sigma = \frac{d+\varepsilon}{2}$ , the dimension of the field  $\phi$  in equation (2.7) becomes  $\Delta_\phi = \frac{d-\varepsilon}{4}$ , so that the  $\phi^4$  interaction is weakly relevant, allowing for a perturbative expansion in  $\varepsilon$ . An important and interesting feature of this expansion is that it can be performed at a fixed  $d$ . The perturbative  $\beta$ -function for the  $\lambda$  coupling has a non-trivial zero, corresponding to an infrared (IR) fixed point. The standard  $\varepsilon$ -expansion procedure can then be used to compute observables at the perturbative fixed point, with the crucial difference that the field  $\phi$ , being non-local, does not renormalize. This is the expansion that was first introduced in [2].
- Following the standard procedure, one can set  $d = 4 - \hat{\varepsilon}$ , while introducing an additional parameter  $\kappa$  such that  $\sigma = 2 - \frac{(1-\kappa)\hat{\varepsilon}}{2}$ . This new parameter defines a specific direction when moving away from the corner  $d = 4$  in figure 1. For  $\kappa = 1$ , we have  $\sigma = 2$ , and the action is local, corresponding to the ordinary SRI fixed point. The opposite limit is  $\kappa = 0$ , where  $\sigma = d/2$ , and one moves along the crossover to the Gaussian theories. All intermediate values  $0 < \kappa < 1$  correspond to the LRI fixed points. A similar expansion has been considered in [6].

A large  $N$  expansion is also possible [61], although it will not be considered in this work. The second expansion is particularly useful in section 4, where we consider the generalization of the localized magnetic field to the long-range model. Here, we focus on the first expansion and briefly review the renormalization procedure.

As mentioned earlier, the kinetic term of the action is non-local, and since renormalization always introduces local counterterms, the field  $\phi$  does not renormalize. This implies that all divergences must be canceled by renormalizing the coupling  $\lambda$ . We can express the renormalized coupling in terms of the bare coupling as  $\lambda_0 = \mu^\varepsilon Z_\lambda \lambda$ , where  $\mu$  is a mass scale. The action

is then written as

$$S = \frac{\mathcal{N}_\sigma}{2} \int d^d x d^d y \frac{\phi_a(x) \phi_a(y)}{|x-y|^{d+\sigma}} + \frac{Z_\lambda \lambda \mu^\varepsilon}{4!} \int d^d x (\phi_a(x) \phi_a(x))^2, \quad (2.10)$$

where  $Z_\lambda$  ensures the cancellation of all poles in  $\varepsilon$  in the correlators of  $\phi$ . At two-loop order, in the MS scheme, one gets

$$Z_\lambda = 1 + \frac{\lambda(N+8)}{3(4\pi)^{\frac{d}{2}} \Gamma(\frac{d}{2}) \varepsilon} + \frac{\lambda^2}{9(4\pi)^d \Gamma(\frac{d}{2})^2} \left( \frac{N+8}{\varepsilon^2} + -\frac{(5N+22)(\psi(\frac{d}{2}) - 2\psi(\frac{d}{4}) - \gamma_E)}{\varepsilon} \right) + \mathcal{O}(\lambda^3). \quad (2.11)$$

The beta function  $\beta_\lambda = \mu \frac{\partial \lambda}{\partial \mu}$  is obtained by imposing  $\mu \frac{d}{d\mu} \lambda_0 = 0$ , and it is [2, 61]

$$\beta_\lambda = -\varepsilon \lambda + \frac{(N+8)\lambda^2}{3(4\pi)^{\frac{d}{2}} \Gamma(\frac{d}{2})} - \frac{2(5N+22)(\psi(\frac{d}{2}) - 2\psi(\frac{d}{4}) - \gamma_E)\lambda^3}{9(4\pi)^d \Gamma(\frac{d}{2})^2} + \mathcal{O}(\lambda^4). \quad (2.12)$$

This beta function has a non-trivial zero, corresponding to a perturbative fixed point

$$\frac{\lambda_*}{\Gamma(\frac{d}{2})(4\pi)^{\frac{d}{2}}} = \frac{3}{N+8} \varepsilon + \frac{6(5N+22)(\psi(\frac{d}{2}) - 2\psi(\frac{d}{4}) - \gamma_E)}{(N+8)^3} \varepsilon^2 + \mathcal{O}(\varepsilon^3). \quad (2.13)$$

The conformal invariance of this long-range  $O(N)$  fixed point can be ascertained by extending the arguments of [13] for the LRI model.

## 2.2. Existence and classification of some non-trivial defects

The goal of this work is the construction of non-trivial conformal defects in the non-local  $O(N)$  model that we have just introduced. As a side result, we will also discuss the existence of non-trivial defects in the particular case  $\lambda = 0$ , i.e. for GFF theories. Indeed, it has been shown that in integer dimensions less than four, free local theories do not admit any non-trivial defects [62], where trivial means Gaussian. We will show that, dropping the assumption of locality, we will be able to construct non-trivial conformal defects for GFF in three dimensions.

We begin by describing the most straightforward defects that can be constructed. The first type is obtained by integrating a power of one of the fields,  $\phi^a$ , along a line, thereby breaking  $O(N)$  symmetry down to  $O(N-1)$ . This is analogous to the localized magnetic field, as discussed in [46, 70]. We will explain why this construction does not lend itself easily to an expansion around  $\sigma = d/2$  at fixed  $d$ , and introduce two alternative strategies to overcome this challenge, which we will refer to as the *semiclassical* and *non-local* defects.

Another simple defect is obtained by integrating the singlet  $\phi_a \phi_a$  over a surface. The analogous defect for the local  $O(N)$  model is discussed in [54–56]. Similar considerations apply in this case as well.

Of course, one could also consider other types of defects, such as magnetic impurities or monodromy defects. However, in this paper, we focus on the simplest constructions.

**2.2.1. Local defects.** As mentioned earlier, the simplest approach to constructing defects is to integrate integer powers of the fields  $\phi_a$  over a  $p$ -dimensional subspace. Thus, we can consider the action

$$S = S_{\text{bulk}} + h_0^{a_1 \dots a_n} \int d^p \tau \phi_{a_1}(\tau) \dots \phi_{a_n}(\tau), \quad (2.14)$$

where  $S_{\text{bulk}}$  is given by (2.4), and  $h_0^{a_1 \dots a_n}$  is a coupling constant. The usual strategy is to compute the beta function for the coupling  $h$  and look for perturbative fixed points in the  $\varepsilon$ -expansion. For the expansion to be reliable, we need the coupling to be classically marginal, which requires  $n\Delta_\phi = p$ . Since the dimension of  $\phi$  is determined by the bulk theory, we have

$$n = \frac{2p}{d - \sigma}. \quad (2.15)$$

At the crossover point  $\sigma = d/2$ , we find  $n = \frac{4p}{d}$ , which, for  $2 \leq d \leq 4$ , is an integer only if  $d = 2$  or  $d = 4$ . For this reason, this construction, unlike the case of the homogeneous long-range  $O(N)$  model, forces us to consider the  $\hat{\varepsilon}$ -expansion around  $d = 4$ , and we cannot work at fixed  $d$ .

In section 3, we will explore the  $\hat{\varepsilon}$ -expansion for the cases  $p = n = 1$  (i.e. the long-range generalization of the localized magnetic field [46, 70]), and  $p = n = 2$  (i.e. the generalization of the surface defects studied in [54, 56]).

**2.2.2. Non-local defects.** One of the main advantages of the non-local model is that it can be studied at fixed  $d$ . Therefore, we would like to find a defect construction that is suitable for the  $\varepsilon$ -expansion near the crossover line  $\sigma = d/2$ . To achieve this, we introduce additional defect degrees of freedom with a non-local defect action, and couple them to the bulk via a local interaction<sup>5</sup>. For simplicity, let us consider the case  $N = 1$ . We introduce an additional bosonic field  $\hat{\psi}$  on the defect and consider the following class of actions:

$$S = \int d^d x \left( \frac{1}{2} \phi \mathcal{L}_\sigma \phi + \frac{\lambda_0}{4!} \phi^4 \right) + \int d^p \tau \left( \frac{1}{2} \hat{\psi} \mathcal{L}_{\hat{\sigma}} \hat{\psi} + \frac{g_0}{2} \phi^a \hat{\psi}^b \right), \quad (2.16)$$

where  $\hat{\sigma} = p - 2\hat{\Delta}_{\hat{\psi}}$ , and  $a$  and  $b$  are integers. We can then tune the dimension  $\hat{\Delta}_{\hat{\psi}}$  so that the coupling  $g_0$  becomes classically marginal. This yields the condition

$$a\Delta_\phi + b\hat{\Delta}_{\hat{\psi}} \sim p, \quad (2.17)$$

where the relation holds up to a small regulator that must be introduced to cure the divergences of the theory. Near the crossover  $\sigma = d/2$ , we find

$$\Delta_\phi \sim \frac{d}{4}, \quad \hat{\Delta}_{\hat{\psi}} \sim \frac{4p - ad}{4b}. \quad (2.18)$$

Note that these dimensions will not receive quantum corrections as one moves away from the crossover, since both kinetic terms are non-local. To further constrain the allowed values of

<sup>5</sup> A similar construction can be found in [66], where free scalar theories are coupled to lower dimensional CFTs living on a defect.

the exponents  $a$  and  $b$ , we impose the unitarity condition

$$\hat{\Delta}_{\hat{\psi}} \geq \max\left(0, \frac{p-2}{2}\right). \quad (2.19)$$

The valid choices of parameters for a unitary theory are summarized below for  $3 \leq d \leq 4$ :

- $p = 1$ :  $a = 1$ , any  $b$
- $p = 2$ :  $a = 1$  or  $2$ , any  $b$

Of course, having a classically marginal defect interaction is not sufficient to produce a non-trivial conformal defect in the IR. While the renormalization of the coupling  $\lambda$  is unaffected by the presence of the defect, one must search for non-trivial fixed points of the coupling  $g$  by computing its beta function and looking for a non-trivial zero. Section 3 will be devoted to this analysis for specific cases with low values of  $a$  and  $b$ . In particular, we will show that these defects are admissible even in the case  $\lambda = 0$ , i.e. for GFF theory in  $d = 3$ .

Moreover, for  $b = 1$  or  $2$ , the defect field  $\hat{\psi}$  can be integrated out in the action (2.16) (see appendix D for details). This leads to an effective action for  $\phi$ , providing an alternative approach to computing correlation functions of  $\phi$ .

**2.2.3. Semiclassical defects.** Another possible strategy for constructing conformal defects at fixed  $d$  in the long-range  $O(N)$  model is to investigate the IR fixed points of defect RG flows triggered by strongly relevant interactions. In general, this is a challenging problem, as the defect couplings are not perturbatively small in this regime. However, in certain cases, it is possible to study a strongly coupled defect in a weakly coupled bulk theory by expanding the action around a classical configuration that corresponds to a saddle point of the path integral. In our case, the classical configuration for the field  $\phi(x)$  must be consistent with the constraints imposed by the defect conformal symmetry. For example, in the case of an  $O(N)$  symmetry-breaking line, we must have

$$\phi_{\text{cl}}^a(x) = \delta_{a1} \frac{\mathcal{N}_\phi a_{\text{cl}}}{|x_\perp|^{\Delta_{\text{cl}}}}. \quad (2.20)$$

The constants  $a_{\text{cl}}$  and  $\Delta_{\text{cl}}$  can be determined by solving the classical equations of motion. The semiclassical expansion

$$\phi^a(x) = \phi_{\text{cl}}^a(x) + \delta\phi^a(x), \quad (2.21)$$

leads to an action for the fluctuation  $\delta\phi$ , which can be used to compute quantum corrections to observables in the defect field theory. This method has been used to study the  $O(N)$  model in the presence of a boundary in various regimes [35, 71–73], and was also considered for surface defects in [56]<sup>6</sup>. However, some technical issues arise when one applies the same techniques to compute quantum corrections in defects with codimension  $q = d - p \neq 1$ . We will discuss this construction in more detail in section 5.

An alternative approach for studying strongly coupled defects in weakly coupled bulks, which we do not pursue in this work, is to use the methods introduced in [60]. By considering a non-integer dimensional defect where the interaction is weakly relevant, it may be possible to compute observables and then extrapolate the results to integer values of the defect dimension.

<sup>6</sup> See also [74, 75] for a similar approach in the context of defects in  $\mathcal{N} = 4$  super Yang-Mills.

### 3. Non-local defects

In this section we begin our analysis of the non-local defects introduced in section 2.2.2. Our goal is to compute the beta function for the defect coupling  $g$  and identify non-trivial perturbative zeros in the  $\varepsilon$ -expansion at fixed  $d$ . We focus primarily on the free bulk case  $\lambda = 0$ , and on the LRI model, i.e.  $N = 1$ . However, most of our results can be straightforwardly generalized to arbitrary  $N$ . Since the construction of these defects is carried out at a fixed dimension  $d$ , this analysis also serves as a study of the existence of non-trivial defects in GFF theory across different dimensions. In particular, we will show that GFF theory in three dimensions admits non-trivial conformal defects. Additionally, we will also show that introducing the bulk interaction, in most cases, does not affect the leading-order results for the beta function or the defect CFT data.

Before examining specific values of the exponents  $(a, b)$  in (2.16), we first establish some general results that hold for all RG flows considered in this section. To begin, we need to specify how we regulate the divergences. We introduce a regulator  $\varepsilon$  and impose that the defect interaction term in (2.16) is weakly relevant

$$a\Delta_\phi + b\hat{\Delta}_{\hat{\psi}} = p - \varepsilon. \tag{3.1}$$

When the bulk theory is free, this choice is sufficient to ensure that all correlators remain finite. In the case of an interacting bulk, we must also specify how to move away from the crossover at  $\sigma = d/2$ . As in section 2.1, we set  $\varepsilon = 2\sigma - d$ , where  $\varepsilon$  now regulates bulk integrals as well. This choice is not unique; we could have inserted an arbitrary coefficient in front of the  $\varepsilon$  in (3.1) (or, alternatively, use two independent regulators). However, as we will show, at leading order in  $\varepsilon$  only defect integrals contribute, and it is straightforward to generalize the results introducing an additional coefficient. With this choice, the relation between the bare and the renormalized defect coupling is

$$g_0 = \mu^\varepsilon Z_g g(\mu), \tag{3.2}$$

and we can use this to compute the beta function.

To compute the beta function, one typically imposes that a given observable is finite by reabsorbing the divergences into the renormalization constants. A commonly used observable for this purpose is the bulk one-point function of the field  $\phi$ . However, in some models that we are considering, the perturbative computation of this one-point function involves tadpole integrals, which complicate the analysis.

Instead, we find it more convenient to look at the defect two-point function of a special composite operator,  $\hat{\mathcal{O}}_0 = \hat{\phi}^{a-1} \hat{\psi}^b$ , which appears in the equation of motion for  $\phi$ . Indeed, in the free bulk case we have

$$\mathcal{L}_\sigma \phi(0, x_\perp) = -\frac{g_0}{2} a \hat{\mathcal{O}}_0(0) \delta^{(d-p)}(x_\perp). \tag{3.3}$$

Since the bulk field  $\phi$  does not renormalize (due to its non-local kinetic term), the left-hand side of (3.3) remains unchanged under renormalization. However, the right-hand side involves the renormalization of the coupling  $g_0 = \mu^\varepsilon Z_g g$  and the wavefunction renormalization of the defect operator  $\hat{\mathcal{O}}_0 = Z_{\hat{\mathcal{O}}} \hat{\mathcal{O}}$ . This implies that in the MS scheme, these two quantities are related by the condition  $Z_g Z_{\hat{\mathcal{O}}} = 1$ . Therefore, the renormalization of the coupling (and the corresponding beta function) can be derived from the wavefunction renormalization of  $\hat{\mathcal{O}}$ . Indeed,

at leading order, we expect the wavefunction renormalization to take the form

$$Z_{\hat{\mathcal{O}}} = 1 - \frac{\alpha g^n}{\varepsilon} + \mathcal{O}(g^{n+1}), \quad (3.4)$$

where  $n$  is an integer related to the values of  $a$  and  $b$ , and  $\alpha$  is a real number. The renormalization factor for the coupling is then given by

$$Z_g = 1 + \frac{\alpha g^n}{\varepsilon} + \mathcal{O}(g^{n+1}), \quad (3.5)$$

and the beta function can be derived, as usual, by requiring that the bare coupling does not depend on the renormalization mass scale, leading to

$$\beta_g = -\varepsilon g + \alpha n g^{n+1} + \mathcal{O}(g^{n+2}). \quad (3.6)$$

The non-trivial zero of the beta function is  $g_*^n = \varepsilon/(\alpha n) + \mathcal{O}(\varepsilon^2)$ . For odd values of  $n$  this equation will always admit a real solution, while for even values of  $n$  the crucial requirement is that  $\alpha$  is positive. At this fixed point, the equation of motion (3.3) implies that the operator  $\hat{\mathcal{O}}$  is protected with dimension

$$\hat{\Delta}_{\hat{\mathcal{O}}} = p - \Delta_\phi. \quad (3.7)$$

This can also be checked by computing explicitly the anomalous dimension  $\gamma_{\hat{\mathcal{O}}}$  which has the exact expression<sup>7</sup>

$$\gamma_{\hat{\mathcal{O}}} = \beta_g \frac{\partial \log Z_{\hat{\mathcal{O}}}}{\partial g} = \beta_g \frac{\partial \log Z_g^{-1}}{\partial g} = \varepsilon - \frac{\beta_g}{g}, \quad (3.8)$$

and the second term vanishes at the fixed point. Using also that  $a\Delta_\phi + b\hat{\Delta}_{\hat{\psi}} = p - \varepsilon$ , we get  $\hat{\Delta}_{\hat{\mathcal{O}}} = (a-1)\Delta_\phi + b\hat{\Delta}_{\hat{\psi}} + \gamma_{\hat{\mathcal{O}}} = p - \Delta_\phi$ , as expected. Therefore, we have

$$\langle \hat{\mathcal{O}}(\tau_1) \hat{\mathcal{O}}(\tau_2) \rangle = \frac{\mathcal{N}_{\hat{\mathcal{O}}}^2}{|\tau_1 - \tau_2|^{p - \Delta_\phi}}, \quad (3.9)$$

where  $\mathcal{N}_{\hat{\mathcal{O}}}$  is a normalization constant.

Furthermore, one can invert the equation of motion to express  $\phi$  in terms of integrals of the operator  $\hat{\mathcal{O}}$  on the defect. This allows to compute bulk correlators of  $\phi$  by integrating defect correlators of  $\hat{\mathcal{O}}$ , without having to compute Feynman diagrams [43]. Indeed, by inverting (3.3), we find

$$\phi(x) = -a \mathcal{N}_\sigma \frac{g_0}{2} \int d^p \tau \frac{\hat{\mathcal{O}}(\tau)}{(|x_\perp|^2 + |\tau|^2)^{\Delta_\phi}} + \phi_{\text{free}}(x), \quad (3.10)$$

where  $\phi_{\text{free}}$  is a free field, which does not interact with the defect. This can be used to compute the one-point function of  $\phi^2$

<sup>7</sup> A useful relation that can be used for this computation is  $\beta_g = \frac{-\varepsilon g Z_g}{Z_g + g \partial_g Z_g}$ .

$$\begin{aligned} \langle \phi^2(x) \rangle &= g_0^2 \frac{a^2 \mathcal{N}_\sigma^2 \mathcal{N}_{\hat{\mathcal{O}}}^2}{4} \int \frac{d^p \tau_1 d^p \tau_2}{(|x_\perp|^2 + |\tau_1|^2)^{\Delta_\phi} |\tau_1 - \tau_2|^{2(p-\Delta_\phi)} (|x_\perp|^2 + |\tau_2|^2)^{\Delta_\phi}} \\ &= g_0^2 \frac{a^2 \mathcal{N}_\sigma^2 \mathcal{N}_{\hat{\mathcal{O}}}^2}{4} \frac{\pi^p \Gamma(\frac{p}{2}) \Gamma(\Delta_\phi - \frac{p}{2})}{\Gamma(\Delta_\phi) (p-1)!} \frac{1}{|x_\perp|^{2\Delta_\phi}} = \frac{a_{\phi^2} \mathcal{N}_{\phi^2}}{|x_\perp|^{2\Delta_\phi}}, \end{aligned} \quad (3.11)$$

where  $\mathcal{N}_{\phi^2} = 2\mathcal{N}_\phi^2$ . The last step to compute a piece of defect CFT data is to evaluate this expression at the fixed point  $g_*$ . We will do this in a few specific cases below.

Similarly, we can compute the bulk-to-defect one-point functions of  $\phi$  and  $\hat{\mathcal{O}}$ , as well as the bulk two-point function of  $\phi$ . For example, consider the correlator  $\langle \phi(x)\phi(y) \rangle$ . Following [43], we can exploit the residual conformal symmetry to set  $x_\parallel = y_\parallel = 0$  and  $x_\perp = (z, \bar{z}, 0, \dots)$ ,  $y_\perp = (0, 1, 0, \dots)$ . It is also convenient to define a radial coordinate by  $z\bar{z} = r$ . Using (3.10) we get

$$\begin{aligned} \langle \phi(0, x_\perp) \phi(0, y_\perp) \rangle &= g_0^2 \frac{a^2 \mathcal{N}_{2\Delta_\phi-d}^2 \mathcal{N}_{\hat{\mathcal{O}}}^2}{4} \\ &\quad \times \int \frac{d^p \tau_1 d^p \tau_2}{(1 + |\tau_1|^2)^{\Delta_\phi} |\tau_1 - \tau_2|^{2(p-\Delta_\phi)} (r^2 + |\tau_2|^2)^{\Delta_\phi}} + G(x-y), \end{aligned} \quad (3.12)$$

where  $G(x-y)$  is the free  $\phi$  propagator. This integral can be computed exactly. By restoring the dependence on arbitrary  $x$  and  $y$  and evaluating at the fixed point, we get




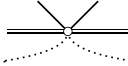
$$\begin{aligned} \langle \phi(x) \phi(y) \rangle &= \frac{\mathcal{N}_\phi^2 F_{\phi\phi}(r)}{|x_\perp|^{\Delta_\phi} |y_\perp|^{\Delta_\phi}}, \\ F_{\phi\phi}(r) &= \xi^{-\Delta_\phi} + g_*^2 \frac{a^2 \mathcal{N}_\sigma^2 \mathcal{N}_{\hat{\mathcal{O}}}^2}{4 \mathcal{N}_\phi^2} \left( \frac{\pi^{p+2} r^{p-\Delta_\phi} {}_2F_1(\frac{p}{2}, p-\Delta_\phi; \frac{p}{2}-\Delta_\phi+1; r^2)}{\Gamma(\Delta_\phi)^2 \sin^2(\pi(\frac{p}{2}-\Delta_\phi)) \Gamma(\frac{p}{2}-\Delta_\phi+1)^2} + \right. \\ &\quad \left. - \frac{2\pi^{p+1} r^{\Delta_\phi} {}_2F_1(\frac{p}{2}, \Delta_\phi; 1-\frac{p}{2}+\Delta_\phi; r^2)}{\Gamma(\Delta_\phi) (p-2\Delta_\phi) \sin(\pi(\frac{p}{2}-\Delta_\phi)) \Gamma(p-\Delta_\phi)} \right), \end{aligned} \quad (3.13)$$

where  $\xi = (x-y)^2/(|x_\perp||y_\perp|)$  is a conformal cross ratio. From (3.13) we can immediately read off the spectrum of the exchanged operators in the defect channel operator product expansion (OPE). The only primary operators are  $(\partial_\perp)^s \phi$  with  $s$  integer and dimension  $\hat{\Delta}_s = 1 + s - \varepsilon/2$ , and the operator  $\hat{\mathcal{O}}$  with dimension  $\Delta_{\hat{\mathcal{O}}} = p - \Delta_\phi$ . one can also easily extract all the bulk-to-defect OPE coefficients for the operators exchanged in the defect channel, as well as the one-point function coefficients for the operators exchanged in the bulk channel, as showed in [43].

In the interacting bulk case, there are non-linear corrections to the left-hand side (3.3) and the above analysis does not apply. However, in the models we consider, corrections due to the bulk coupling only appear at next-to-leading order. As a result, the above results remain valid perturbatively at leading order in  $\varepsilon$ .

We are now ready to compute the wavefunction renormalization  $Z_{\hat{\mathcal{O}}}$  for some of the models discussed in section 2.2.2 by looking at the two-point function  $\langle \hat{\mathcal{O}} \hat{\mathcal{O}} \rangle$  using Feynman diagrams. This will enable us to compute the beta function and identify perturbative fixed points. Specifically, we will consider the cases  $(a, b) = (1, 2)$ ,  $(a, b) = (2, 1)$ , and  $(a, b) = (2, 2n)$ . Moreover, we will also prove that for a line defect and  $1/2 < \Delta_\phi < 1$ , there exists a real fixed point for arbitrary  $b$ .

**Table 1.** Feynman rules for the non-local defect.

Element	Rule
	$\phi$ propagator: $G(x-y) = \frac{\mathcal{N}_\phi^2}{ x-y ^{2\Delta_\phi}}$
	$\hat{\psi}$ propagator: $G(x-y) = \frac{\mathcal{N}_{\hat{\psi}}^2}{ x-y ^{2\hat{\Delta}_{\hat{\psi}}}}$
	Bulk $\phi^4$ interaction $-\frac{\lambda_0}{4!} \int d^d x$ , where $x$ is the interaction point
	Defect $\phi^a \hat{\psi}^b$ interaction $-\frac{g_0}{2} \int d^p \tau$ , where $\tau$ is the interaction point on the defect

Let us summarize the conventions used for the Feynman diagrams throughout this paper. A blue line always represents a defect: a straight blue line corresponds to a linear defect (a line defect, a surface, etc), while a blue circle represents a circular or (hyper)spherical defect. Solid black lines denote the field that is defined both in the bulk and on the defect (denoted by  $\phi$ ), whereas dotted lines represent a field defined only on the defect (denoted by  $\hat{\psi}$ ). We will use the following normalization constants

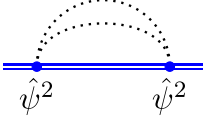
$$\mathcal{N}_\phi^2 = \frac{\Gamma(\Delta_\phi)}{2^{d-2\Delta_\phi} \pi^{\frac{d}{2}} \Gamma(\frac{d}{2} - \Delta_\phi)}, \quad \mathcal{N}_{\hat{\psi}}^2 = \frac{\Gamma(\hat{\Delta}_{\hat{\psi}})}{2^{p-2\hat{\Delta}_{\hat{\psi}}} \pi^{\frac{p}{2}} \Gamma(\frac{p}{2} - \hat{\Delta}_{\hat{\psi}})}. \quad (3.14)$$

Feynman rules are summarized in table 1. Additionally, we find it useful to define the following function [13]

$$w_\alpha^{(d)} = (4\pi)^{\frac{d}{2}} 2^{-\alpha} \frac{\Gamma(\frac{d-\alpha}{2})}{\Gamma(\frac{\alpha}{2})}. \quad (3.15)$$

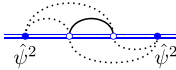
3.1.  $(a,b) = (1,2)$

We start from  $(a,b) = (1,2)$  in the free bulk case. The interaction term in (2.16) becomes  $\frac{g_0}{2} \int d^p \tau \phi \hat{\psi}^2$ . The operator  $\hat{O}$  in this case is  $\hat{O} = \hat{\psi}^2$ . The bare two-point function  $\langle \hat{O} \hat{O} \rangle$  at tree level is given by the following diagram



$$= \frac{2(\mathcal{N}_{\hat{\psi}}^2)^2}{|\tau|^{4\hat{\Delta}_{\hat{\psi}}}}. \quad (3.16)$$

At one loop, there are three diagrams, but only one turns out to be divergent. Since we only need to compute  $Z_{\hat{O}}$ , it suffices to consider this diagram



$$= \mathcal{N}_\phi^2 (\mathcal{N}_{\hat{\psi}}^2)^4 g_0^2 \int \frac{d^p \tau_1 d^p \tau_2}{(|\tau_1| |\tau_2| |\tau - \tau_1| |\tau - \tau_2|)^{2\hat{\Delta}_{\hat{\psi}}} |\tau_2 - \tau_1|^{2\Delta_\phi}}. \quad (3.17)$$

The divergent part of this diagram can be easily extracted by analyzing the limits  $\tau_1, \tau_2 \rightarrow 0, \tau$

$$\begin{aligned}
 \text{Diagram} &= \frac{\mathcal{N}_\phi^2 (\mathcal{N}_{\hat{\psi}}^2)^4 g_0^2}{|\tau|^{4\Delta_\psi}} \left( \frac{w_{2\Delta_\phi}^{(p)} w_{2\hat{\Delta}_{\hat{\psi}}}^{(p)}}{w_{2\Delta_\phi+2\hat{\Delta}_{\hat{\psi}}-p}^{(p)}} \frac{2\pi^{\frac{p}{2}}}{\Gamma(\frac{p}{2})} \frac{1}{\varepsilon} + \mathcal{O}(\varepsilon^0) \right). \quad (3.18)
 \end{aligned}$$

This divergence must be canceled by introducing the wavefunction renormalization  $Z_{\hat{\psi}}$ . Then, using (3.6), we can extract the beta function and the fixed point  $g_*$

$$\begin{aligned}
 Z_{\hat{\psi}} &= 1 + g^2 \frac{\Gamma(\frac{p}{2} - \Delta_\phi)}{2^{d+1} \pi^{\frac{d}{2}} \Gamma(\frac{p}{2}) \Gamma(\frac{d}{2} - \Delta_\phi)} \varepsilon + \mathcal{O}(g^4), \\
 \beta_g &= -\varepsilon g - \frac{\Gamma(\frac{p}{2} - \Delta_\phi)}{2^d \pi^{\frac{d}{2}} \Gamma(\frac{p}{2}) \Gamma(\frac{d}{2} - \Delta_\phi)} g^3 + \mathcal{O}(g^4), \\
 g_*^2 &= -\frac{2^d \pi^{\frac{d}{2}} \Gamma(\frac{p}{2}) \Gamma(\frac{d}{2} - \Delta_\phi)}{\Gamma(\frac{p}{2} - \Delta_\phi)} \varepsilon + \mathcal{O}(\varepsilon^2). \quad (3.19)
 \end{aligned}$$

Notice that the fixed-point coupling  $g_*$  is not necessarily real. Interestingly, when  $d = p + 2$ , we find that  $g_*^2 > 0$  for any  $\Delta_\phi$  above the unitarity bound. In the general case, only certain ranges of  $\Delta_\phi$  yield a real fixed point.

Using (3.11), we can also extract the one-point function of  $\phi^2$

$$a_{\phi^2} = -\frac{9 \Gamma(\frac{p}{2})^2 \Gamma(\Delta_\phi - \frac{p}{2}) \Gamma(\frac{p-\Delta_\phi}{2})^2}{8 \Gamma(\frac{\Delta_\phi}{2})^2 \Gamma(\frac{p}{2} - \Delta_\phi) (p-1)!} \varepsilon + \mathcal{O}(\varepsilon^2). \quad (3.20)$$

In summary, we find that the interaction term  $\phi \hat{\psi}^2$  provides a non-trivial defect CFT for some values of  $p, d$ , and  $\Delta_\phi$ . Specifically, for  $d = 3$  and  $p = 1$ , we find a perturbative fixed point at

$$g_*^2 = 2\pi^2 \varepsilon + \mathcal{O}(\varepsilon^2). \quad (3.21)$$

Notice that we have not taken into account the bulk interaction here; therefore, we explicitly constructed an example of a non-trivial conformal defect in three-dimensional GFF theory. In this picture,  $\Delta_\phi$  is a free parameter.

One may also wonder what the effect of introducing the bulk interaction would be. We can easily see that this effect would only contribute at higher orders in  $\varepsilon$  for the beta function. However, in this case,  $\Delta_\phi$  is no longer a free parameter, because we must take  $\Delta_\phi = (d - \varepsilon)/4$ .<sup>8</sup> For  $d = 3$ , the fixed point with  $p = 1$  is the only real one, since  $p = 2$  yields a negative value for  $g_*^2$ .

### 3.2. $(a, b) = (2, 1)$

The second case we analyze is  $(a, b) = (2, 1)$ , with interaction term  $\frac{g_0}{2} \int d^p \tau \phi^2 \hat{\psi}$ . Again, we first consider the free bulk case. The operator  $\hat{\mathcal{O}}$  is given by  $\hat{\mathcal{O}} = \phi \hat{\psi}$ , and the tree-level contribution to its bare two-point function is given by

$$\begin{aligned}
 \text{Diagram} &= \frac{\mathcal{N}_\phi^2 \mathcal{N}_{\hat{\psi}}^2}{|\tau|^{2(\Delta_\phi + \hat{\Delta}_{\hat{\psi}})}}. \quad (3.22)
 \end{aligned}$$

<sup>8</sup> Up to an arbitrary positive coefficient in front of  $\varepsilon$ , as it was discussed at the beginning of section 3.

Again, at one loop there is only one divergent diagram, whose divergent can be computed as before

$$\begin{aligned}
 \text{Diagram} &= \frac{(\mathcal{N}_\phi^2)^3 (\mathcal{N}_\psi^2)^2 g_0^2}{|\tau|^{2\Delta_\phi + 2\hat{\Delta}_\psi}} \left( \frac{w_{2\Delta_\phi}^{(p)} w_{2\hat{\Delta}_\psi}^{(p)}}{w_{2\Delta_\phi + 2\hat{\Delta}_\psi - p}^{(p)}} \frac{2\pi^{\frac{p}{2}}}{\Gamma(\frac{p}{2})} \frac{1}{\varepsilon} + \mathcal{O}(\varepsilon^0) \right). \quad (3.23)
 \end{aligned}$$

This yields the following renormalization factor, beta functions and fixed point

$$\begin{aligned}
 Z_{\hat{\mathcal{O}}} &= 1 + \frac{\Gamma(\frac{p}{2} - \Delta_\phi)^2 g^2}{2^{2d-p-1} \pi^{d-\frac{p}{2}} \Gamma(\frac{p}{2}) \Gamma(\frac{d}{2} - \Delta_\phi)^2 \varepsilon} + \mathcal{O}(g^4), \\
 \beta_g &= -\varepsilon g - \frac{\Gamma(\frac{p}{2} - \Delta_\phi)^2}{2^{2(d-1)-p} \pi^{d-\frac{p}{2}} \Gamma(\frac{p}{2}) \Gamma(\frac{d}{2} - \Delta_\phi)^2} g^3 + \mathcal{O}(g^4), \\
 g_*^2 &= -\frac{2^{2(d-1)-p} \pi^{d-\frac{p}{2}} \Gamma(\frac{p}{2}) \Gamma(\frac{d}{2} - \Delta_\phi)^2}{\Gamma(\frac{p}{2} - \Delta_\phi)^2} \varepsilon + \mathcal{O}(\varepsilon^2). \quad (3.24)
 \end{aligned}$$

In this case, we find that the fixed-point value  $g_*^2$  is always negative. Therefore, we cannot find any real fixed point. Moreover, as in the previous case, the situation does not change at leading order when the bulk interactions are turned on.

### 3.3. $(a, b) = (2, 2n)$

The last case that we analyze explicitly is the family given by  $a = 2$  and  $b = 2n$  even. The interaction term in (2.16) becomes  $\frac{g_0}{2} \int d^p \tau \phi^2 \hat{\psi}^{2n}$ . The operator  $\hat{\mathcal{O}}$  in this case is  $\hat{\mathcal{O}} = \phi \hat{\psi}^{2n}$ . The tree-level bare two-point function is given by the following diagram

$$\begin{aligned}
 \text{Diagram} &= \frac{(2n)! \mathcal{N}_\phi^2 (\mathcal{N}_\psi^2)^{2n}}{|x|^{2\Delta_\phi + 4n\hat{\Delta}_\psi}}, \quad (3.25)
 \end{aligned}$$

where the dotted line with the label  $2n$  represents  $2n$  propagators of  $\hat{\psi}$ . At one loop, there is only one divergent diagram. Since we only need to compute  $Z_{\hat{\mathcal{O}}}$ , it suffices to consider the following diagram

$$\begin{aligned}
 \text{Diagram} &= -\frac{g_0}{2} 2 \binom{2n}{n}^2 n! (2n)! (\mathcal{N}_\phi^2)^2 (\mathcal{N}_\psi^2)^{3n} \frac{\left( \frac{w_{2\Delta_\phi + 2n\hat{\Delta}_\psi}^{(p)}}{w_{4\Delta_\phi + 4n\hat{\Delta}_\psi - p}^{(p)}} \right)^2}{|x|^{4\Delta_\phi + 6n\hat{\Delta}_\psi - p}}. \quad (3.26)
 \end{aligned}$$

The above quantity diverges as  $\varepsilon \rightarrow 0$ , and the corresponding pole must be canceled by introducing the wavefunction renormalization  $Z_{\hat{\phi}}$ . Then, using (3.6), we can extract the beta function and the fixed point  $g_*$

$$\begin{aligned} Z_{\hat{\phi}} &= 1 - \frac{g}{\varepsilon} \frac{2^{1+2\Delta_\phi - p} ((2n)!)^2 \Gamma(\Delta_\phi)}{(4\pi)^{\frac{d-p}{2}} n! \Gamma(\frac{d}{2} - \Delta_\phi) \Gamma(\frac{p}{2})} \left( \frac{4^{\frac{p-2\Delta_\phi}{2n}} \Gamma(\frac{p-2\Delta_\phi}{2n})}{(4\pi)^{\frac{p}{2}} \Gamma(\frac{p}{2} - \frac{p-2\Delta_\phi}{2n})} \right)^n + \mathcal{O}(g^2), \\ \beta_g &= -\varepsilon g + \frac{2^{1+2\Delta_\phi - p} ((2n)!)^2 \Gamma(\Delta_\phi)}{(4\pi)^{\frac{d-p}{2}} n! \Gamma(\frac{d}{2} - \Delta_\phi) \Gamma(\frac{p}{2})} \left( \frac{4^{\frac{p-2\Delta_\phi}{2n}} \Gamma(\frac{p-2\Delta_\phi}{2n})}{(4\pi)^{\frac{p}{2}} \Gamma(\frac{p}{2} - \frac{p-2\Delta_\phi}{2n})} \right)^n g^2 + \mathcal{O}(g^3), \\ g_* &= \frac{(4\pi)^{\frac{d-p}{2}} n! \Gamma(\frac{d}{2} - \Delta_\phi) \Gamma(\frac{p}{2})}{2^{1+2\Delta_\phi - p} ((2n)!)^2 \Gamma(\Delta_\phi)} \left( \frac{(4\pi)^{\frac{p}{2}} \Gamma(\frac{p}{2} - \frac{p-2\Delta_\phi}{2n})}{4^{\frac{p-2\Delta_\phi}{2n}} \Gamma(\frac{p-2\Delta_\phi}{2n})} \right)^n \varepsilon + \mathcal{O}(\varepsilon^2). \end{aligned} \tag{3.27}$$

Using (3.11), we can also extract the one-point function of  $\phi^2$

$$a_{\phi^2} = \frac{n! \Gamma(\Delta_\phi - \frac{p}{2}) \Gamma(\frac{p}{2})^3}{8\Delta_\phi ((2n)!)^3 (p-1)!} \varepsilon^2 + \mathcal{O}(\varepsilon^3). \tag{3.28}$$

The physically interesting case is  $d = 3, p = 2$  and  $\Delta_\phi = d/4 = 3/4$ . This yields the following expression:

$$g_* = \frac{2^{2n} \sqrt{\pi} n!}{((2n)!)^2} \Gamma\left(1 - \frac{1}{4n}\right)^n \sin^n\left(\frac{\pi}{n}\right) \varepsilon + \mathcal{O}(\varepsilon^2). \tag{3.29}$$

Notice that the fixed point exists for any  $n$  (that is for any even  $b$ ) above.

As in the discussion of the  $(a, b) = (1, 2)$  case, we have not turned on the bulk interaction yet, meaning that these examples provide non-trivial surface defects in three-dimensional GFF theory. If we were to include the bulk interaction, it would still not affect the leading-order computation.

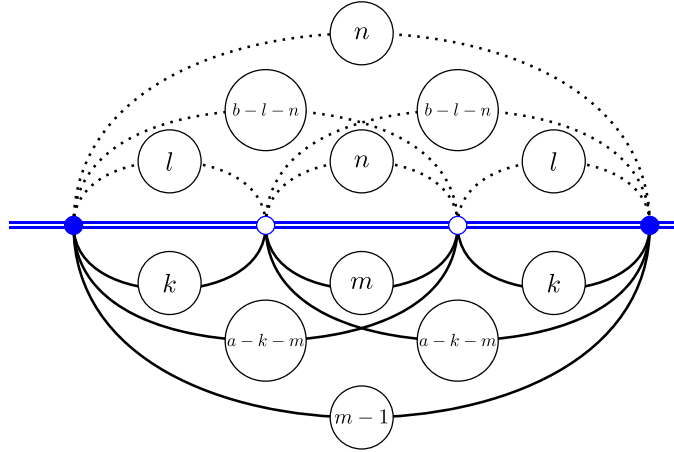
### 3.4. $a$ odd or $b$ odd

As in the cases of  $(a, b) = (1, 2)$  and  $(a, b) = (2, 1)$  which we explicitly worked out previously, we need to go to order  $\mathcal{O}(g_0^2)$  to get divergences. The relevant diagrams thus have two external insertions of  $\phi^{a-1}\psi^b$  and two interaction vertices  $\phi^a\psi^b$ . In order to figure out which diagrams diverge, we can characterize a given diagram by four numbers, say  $k, l, m, n$ , counting various propagators. Our conventions are summarized in figure 2.

Poles in  $\varepsilon$  are likely to appear when all internal vertices are superimposed with one of the external vertices, and a diagram will diverge provided it involves an integral going like

$$\int \frac{d^p \tau}{|\tau|^{2a\Delta_\phi + 2b\Delta_\psi - p}}. \tag{3.30}$$

To obtain this behavior for a given set of  $(k, l, m, n)$ , we can connect the external vertices to the internal ones as many times as possible, before connecting the former to each other using the remaining propagators. Hence the diagrams we consider here involve the following integral



**Figure 2.** General divergent diagram for  $a$  odd or  $b$  odd. A single line stands for multiple propagators of a given type, the number of which being indicated on top of the line in question.

(ignoring combinatorics, which will in fact prove quite tricky):

$$D = \frac{g_0^2}{4|\tau|^{2(m-1)\Delta_\phi + 2n\Delta_\psi}} \times \int \frac{d^p \tau_1 d^p \tau_2}{(|\tau_1||\tau_2 - \tau|)^{2k\Delta_\phi + 2l\Delta_\psi} (|\tau_2||\tau_1 - \tau|)^{2(a-m-k)\Delta_\phi + 2(b-n-l)\Delta_\psi} |\tau_1 - \tau_2|^{2m\Delta_\phi + 2n\Delta_\psi}}, \quad (3.31)$$

where we also omit propagator normalizations for brevity, although they will be restored at the end. Next, let us extract divergences from  $D$ . When  $\tau_1, \tau_2 \rightarrow 0$

$$D \sim \frac{g_0^2}{4|\tau|^{2(a-1)\Delta_\phi + 2b\Delta_\psi}} \times \int \frac{d^p \tau_1 d^p \tau_2}{|\tau_1|^{2k\Delta_\phi + 2l\Delta_\psi} |\tau_2|^{2(a-m-k)\Delta_\phi + 2(b-n-l)\Delta_\psi} |\tau_1 - \tau_2|^{2m\Delta_\phi + 2n\Delta_\psi}}. \quad (3.32)$$

This can now easily be integrated and gives

$$D \sim \frac{g_0^2}{4|\tau|^{2(a-1)\Delta_\phi + 2b\Delta_\psi}} \frac{w_{2m\Delta_\phi + 2n\Delta_\psi}^{(p)} w_{2k\Delta_\phi + 2l\Delta_\psi}^{(p)}}{w_{2(m+k)\Delta_\phi + 2(n+l)\Delta_\psi - p}^{(p)}} \int \frac{d^p \tau_2}{|\tau_2|^{2a\Delta_\phi + 2b\Delta_\psi - p}} \sim \frac{g_0^2}{4|\tau|^{2(a-1)\Delta_\phi + 2b\Delta_\psi}} \frac{w_{2m\Delta_\phi + 2n\Delta_\psi}^{(p)} w_{2k\Delta_\phi + 2l\Delta_\psi}^{(p)}}{w_{2(m+k)\Delta_\phi + 2(n+l)\Delta_\psi - p}^{(p)}} \frac{\pi^{\frac{p}{2}}}{\Gamma(\frac{p}{2}) \varepsilon}. \quad (3.33)$$

Now let us define  $S_{k,l,m,n}$  as the multiplicity of diagrams with given  $(k, l, m, n)$ . The final singular contribution at  $O(g_0^2)$  is hence (adding a factor of two for interaction vertices superimposed on each external vertex)

$$D = \frac{(\mathcal{N}_\phi^2)^{2a-1} (\mathcal{N}_\psi^2)^{2b} \pi^{\frac{p}{2}} g_0^2}{2\Gamma(\frac{p}{2}) \varepsilon |\tau|^{2(a-1)\Delta_\phi + 2b\Delta_\psi}} \sum_{k,l,m,n} S_{k,l,m,n} \frac{w_{2m\Delta_\phi + 2n\Delta_\psi}^{(p)} w_{2k\Delta_\phi + 2l\Delta_\psi}^{(p)}}{w_{2(m+k)\Delta_\phi + 2(n+l)\Delta_\psi - p}^{(p)}}. \quad (3.34)$$

Treating the complicated sum as a black box, by defining it as being some function  $S(p, a, b)$ , we can extract the  $\beta$ -function for this theory

$$\beta_g = -\varepsilon g - \frac{S(p, a, b) \pi^{\frac{p}{2}}}{2(a-1)!b!\Gamma(\frac{p}{2})} \left( \frac{4^{\Delta_\phi} \Gamma(\Delta_\phi)}{(4\pi)^{\frac{d}{2}} \Gamma(\frac{d}{2} - \Delta_\phi)} \right)^a \left( \frac{4^{\frac{p-a\Delta_\phi}{b}} \Gamma(\frac{p-a\Delta_\phi}{b})}{(4\pi)^{\frac{p}{2}} \Gamma(\frac{p}{2} - \frac{p-a\Delta_\phi}{b})} \right)^b g^3. \tag{3.35}$$

Therefore, there exists a non-trivial real fixed point if and only if  $S(p, a, b) < 0$ . Notice that this is in general a non-trivial check, which is sensitive to the combinatorics and to the relative signs of the integrals (the  $w$  factors).

### 3.5. The line defect for general $b$

It turns out that something very special happens for  $p = 1$ , i.e. the line defect, and general  $b$  (recall this implies  $a = 1$  by unitarity). Indeed, all of the integrals turn out to have a negative sign, which combined with the positive combinatorics leads to  $S(1, 1, b) < 0$  and thus to the existence of a fixed point. For those values, we necessarily have  $m = 1$  and  $k = 0$ , and the  $(l, n)$ -dependent integrals yield the following contribution

$$\frac{w_{2m\Delta_\phi+2n\Delta_\psi}^{(p)} w_{2k\Delta_\phi+2l\Delta_\psi}^{(p)}}{w_{2(m+k)\Delta_\phi+2(n+l)\Delta_\psi-p}^{(p)}} = \frac{\sqrt{\pi} \Gamma\left(\frac{b-2l+2l\Delta_\phi}{2b}\right) \Gamma\left(\frac{b-2n+2(n-b)\Delta_\phi}{2b}\right) \Gamma\left(-\frac{(l+n)(\Delta_\phi-1)}{b} + \Delta_\phi - \frac{1}{2}\right)}{\Gamma\left(\frac{l-l\Delta_\phi}{b}\right) \Gamma\left(\frac{n+(b-n)\Delta_\phi}{b}\right) \Gamma\left(-\frac{(b-l-n)(\Delta_\phi-1)}{b}\right)}. \tag{3.36}$$

If we make the reasonable assumption that  $1/2 \leq \Delta_\phi \leq 1$ , which expresses the unitarity constraints and the fact that we do not stray too far from the LRI crossover, then all of the  $\Gamma$ -factors above are positive except for

$$\Gamma\left(\frac{b-2n+2(n-b)\Delta_\phi}{2b}\right) < 0, \tag{3.37}$$

and we get a fixed point

$$g_*^2 = -\frac{2\pi^{b+\frac{d}{2}} \Gamma(b+1) 2^{d-2\Delta_\phi} \Gamma(\frac{d}{2} - \Delta_\phi)}{S(1, 1, b) \Gamma(\Delta_\phi) \cos^b\left(\frac{\pi-\pi\Delta_\phi}{b}\right) \Gamma\left(\frac{2-2\Delta_\phi}{b}\right)^b} > 0. \tag{3.38}$$

### 3.6. Summary

We can summarize our findings for the physically interesting case of  $d = 3$ . In this case, we can have two types of defects: lines and surfaces.

- For  $p = 1$ , the allowed interaction terms are of the form  $\phi \hat{\psi}^b$ . We studied the case  $b = 2$  in GFF theory extensively, finding the existence of a non-trivial line defect. Moreover, we argued that, at leading order, the bulk interaction does not affect this result. Additionally, we have shown that for  $1/2 < \Delta_\phi < 1$ , there exists a real fixed point regardless of the value of  $b$ .

- For  $p = 2$ , we can have interactions  $\phi \hat{\psi}^b$  and  $\phi^2 \hat{\psi}^b$ . We addressed the first case with  $b = 2$  and the second case for  $b = 2n$  even, finding a non-trivial defect only for the second family of interactions. Again, at leading order, the bulk interaction does not affect this result. Unfortunately, for a surface defect and  $a = 1$  or  $2$ , the integrals contribute with poles of alternating sign depending on  $k, l, n, m$ , which, coupled to combinatorics, makes it difficult to study the existence of a real fixed point for general  $b$ .

Of course, for higher values of  $b$ , other potentially interesting defect examples could arise. It would also be interesting to investigate whether there are additional constraints on the allowed values of  $b$ . We leave this analysis for future work.

#### 4. Defects in the long-range $O(N)$ model close to four dimensions

In this section, we discuss the generalization of two simple defects that can be constructed in the short-range  $O(N)$  model, starting from the UV theory in  $d = 4$  and expanding around  $d = 4 - \hat{\varepsilon}$ . Unlike the previous section, where we worked at fixed  $d$  by varying the dimension of the scalar field  $\Delta_\phi$ , here we need to expand around  $d = 4$  for the defect action to be weakly relevant.

To explore the LRI fixed points, in section 2.1 we introduced a parameter  $0 < \kappa < 1$ , with  $\sigma = 2 - \frac{(1-\kappa)\hat{\varepsilon}}{2}$ . This parameterizes a straight line in the  $(d, \sigma)$  plane, where  $\kappa$  selects a particular direction in the phase space shown in figure 1. In general, the LRI fixed points in the  $(d, \sigma)$  plane are characterized by the exact relation  $\Delta_\phi = \frac{d-\sigma}{2}$ . When performing calculations near the local theory in  $d = 4$ , non-vanishing contributions to the wavefunction renormalization and the anomalous dimension of the field  $\phi$  arise. Therefore, by enforcing the condition above, we obtain the following expression for  $\sigma$ :

$$\sigma = d - 2\Delta_\phi = 2 + \frac{\kappa - 1}{2}\hat{\varepsilon} + 2\gamma_\phi(\kappa, \hat{\varepsilon}), \quad (4.1)$$

where  $\gamma_\phi(\kappa, \hat{\varepsilon})$  is the anomalous dimension of the field  $\phi$ , which starts at  $O(\hat{\varepsilon}^2)$ . This parameterizes a one-parameter family of trajectories, ranging from  $\kappa = 0$ , where  $\gamma_\phi(0, \hat{\varepsilon}) = 0$  and  $\sigma = d/2$ , to  $\kappa = 1$ , where  $\gamma_\phi(1, \hat{\varepsilon}) = \gamma_{\text{SRI}}$  and the trajectories approach the upper bound of the LRI region, as shown in figure 1.

By making a simple generalization of the computation for the SRI (or  $\kappa = 1$ ), we can obtain these trajectories at order  $\varepsilon^2$ . Note that, at this stage, we are only considering the homogeneous theory, without any defect. The first contribution to the renormalization of the field  $\phi$  appears at two loops, and it gives:

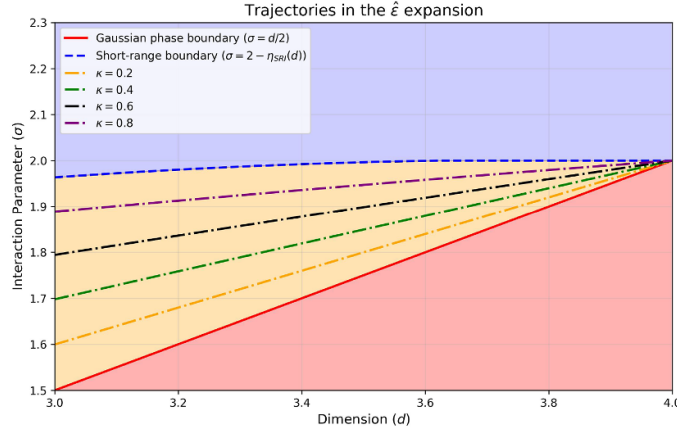
$$Z_\phi = 1 - \frac{(N+2)\lambda^2}{18(4\pi)^4(1+3\kappa)\hat{\varepsilon}} + O(\lambda^3), \quad (4.2)$$

while the coupling renormalization yields

$$Z_\lambda = 1 + \frac{N+8}{3\kappa\hat{\varepsilon}} \frac{\lambda}{(4\pi)^2} + \left( \frac{(N+8)^2}{9\kappa^2\hat{\varepsilon}^2} - \frac{5N+22+\kappa(13N+62)}{9(1+3\kappa)\kappa\hat{\varepsilon}} \right) \frac{\lambda^2}{(4\pi)^4} + O(\lambda^3). \quad (4.3)$$

This leads to the following beta function:

$$\beta_\lambda = -\kappa\hat{\varepsilon}\lambda + \frac{N+8}{3} \frac{\lambda^2}{(4\pi)^2} - \frac{10N+44+\kappa(26N+124)}{9(1+3\kappa)} \frac{\lambda^3}{(4\pi)^4} + O(\lambda^4), \quad (4.4)$$



**Figure 3.** The trajectories  $\sigma(d)$  such that the condition  $\sigma = d - 2\Delta_\phi$  is enforced.

which admits a non-trivial (Wilson–Fisher) fixed point at

$$\frac{\lambda_*}{(4\pi)^2} = \frac{3}{N+8}\kappa\hat{\epsilon} + \frac{6}{(N+8)^3} \frac{5N+22+\kappa(13N+62)}{1+3\kappa} \kappa^2\hat{\epsilon}^2 + \mathcal{O}(\hat{\epsilon}^3). \quad (4.5)$$

From these computations one can immediately derive the anomalous dimension  $\gamma_\phi$  of  $\phi_a$  at the IR fixed point

$$\gamma_\phi = \beta_\lambda \frac{\partial \ln Z_\phi}{\partial \lambda} \Big|_{\lambda=\lambda_*} = \frac{\kappa^3(N+2)}{(1+3\kappa)(N+8)^2} \hat{\epsilon}^2 + \mathcal{O}(\hat{\epsilon}^3). \quad (4.6)$$

This leads to the following family of curves in the  $(d, \sigma)$  plane

$$\sigma = 2 + \frac{\kappa-1}{2}\hat{\epsilon} - \frac{2\kappa^3(N+2)}{(3\kappa+1)(N+8)^2} \hat{\epsilon}^2 + \mathcal{O}(\hat{\epsilon}^3). \quad (4.7)$$

Some of these trajectories are shown in figure 3. As a consistency check, one can easily verify that at  $\kappa = 1$  one retrieves the expressions for the short-range  $O(N)$  model

$$\sigma = 2 - \frac{(N+2)}{2(N+8)^2} \hat{\epsilon}^2 = 2 - \eta_{\text{SRI}}. \quad (4.8)$$

Another useful check, which may be more trivial in flows that do not depend on an extra parameter like  $\kappa$ , is the stability of the bulk IR fixed point. This involves studying the sign of the derivative of  $\beta_\lambda$  at  $\lambda_*$  and ensuring it is positive

$$\beta'_\lambda(\lambda_*) = \kappa\hat{\epsilon} - \frac{2(5N+22+\kappa(13N+62))}{(1+3\kappa)(N+8)^2} \kappa^2\hat{\epsilon}^2 + \mathcal{O}(\hat{\epsilon}^3). \quad (4.9)$$

This leads to the following consistency condition:

$$\hat{\epsilon} < \hat{\epsilon}_{\text{thresh}} = \frac{(1+3\kappa)(N+8)^2}{2\kappa(5N+22+\kappa(13N+62))}. \quad (4.10)$$

For  $0 < \kappa < 1$ , this threshold value is always greater than 1, meaning that this stability condition is never a concern for our perturbative treatment.

#### 4.1. Localized magnetic field

We consider now the insertion of defects in the setup described above. The simplest defect one can consider is the localized magnetic field

$$S = S_0 + h_0 \int d\tau \phi_1(\tau), \quad (4.11)$$

where a single field  $\phi_1$  is integrated along a line. We would like to analyze the renormalization of the coupling  $h$  in the  $\hat{\varepsilon}$ -expansion. We follow the method described in [76] imposing finiteness of the one-point function of  $\phi_1$ . The computation is analogous to the local case, up to the appearance of the new parameter  $\kappa$ . The relevant diagrams are shown in appendix A. The final result for the coupling renormalization  $Z_h$  is

$$Z_h = 1 + \frac{h^2}{3(1+3\kappa)\hat{\varepsilon}} \frac{\lambda}{(4\pi)^2} + \left[ \frac{(N+2)h}{18(1+3\kappa)\hat{\varepsilon}} + \left( \frac{1}{\hat{\varepsilon}^2} - \frac{1+3\kappa^2 - (1-\kappa)(\gamma_E - \log 4\pi)}{4\kappa\hat{\varepsilon}} \right) \frac{2(N+8)h^2}{9(1+3\kappa)(1+5\kappa)} \right. \\ \left. + \left( \frac{2}{(1+3\kappa)\hat{\varepsilon}^2} - \frac{1}{\hat{\varepsilon}} \right) \frac{h^4}{12(1+3\kappa)} \right] \frac{\lambda^2}{(4\pi)^4} + \mathcal{O}(\lambda^3). \quad (4.12)$$

This subsequently yields the following beta function<sup>9</sup>

$$\beta_h = -\frac{\hat{\varepsilon}(1+\kappa)}{4}h + \frac{\lambda}{(4\pi)^2} \frac{h^3}{6} + \frac{\lambda^2}{(4\pi)^4} \left( \frac{(N+2)\kappa h}{9(1+3\kappa)} \right. \\ \left. - \frac{(N+8)(1+3\kappa^2 - (1-\kappa)(\gamma_E - \log(4\pi)))}{36\kappa(1+3\kappa)} h^3 - \frac{h^5}{12} \right) + \mathcal{O}(\lambda^3). \quad (4.13)$$

This beta function reduces to the short range result in the limit  $\kappa \rightarrow 1$  (see for instance [46]). The opposite limit,  $\kappa \rightarrow 0$ , is subtle because in (4.12) the single pole in  $\hat{\varepsilon}$  is accompanied by a single pole in  $\kappa = 0$ , leading to a singular limit  $\kappa \rightarrow 0$  for the beta function (4.13). This pole is cancelled when we set the bulk coupling to the fixed point  $\lambda_*$  in (4.5). In that case, the limit  $\kappa \rightarrow 0$  trivially leads to  $\beta_h = -\hat{\varepsilon}h/4$ , consistently with a Gaussian fixed point. For general  $\kappa$ , instead one has a non-trivial defect fixed point

$$h_*^2 = \frac{(N+8)(1+\kappa)}{2\kappa} + \frac{(5+2(1-\kappa^2)(\log(4\pi) - \gamma_E))(N+8)}{8\kappa(1+3\kappa)} \hat{\varepsilon} \\ + \frac{(15\kappa^2 + 27\kappa + 17)N^2 + 8(15\kappa^2 + 36\kappa + 29)N + 48(9\kappa^2 + 22\kappa + 19)}{8(1+3\kappa)(N+8)} \hat{\varepsilon} + \mathcal{O}(\hat{\varepsilon}^2). \quad (4.14)$$

We now proceed to compute some defect observables at this fixed point.

<sup>9</sup> One should not be worried about the appearance of terms like  $\gamma_E$  or  $\log 4\pi$ , since two-loop coefficients of the beta function for multiple couplings are scheme dependent.

**Scaling dimension.** The first observable that we can compute is the scaling dimension of the defect field  $\hat{\phi}_1$ . This is just a derivative of the beta function:  $\Delta_{\hat{\phi}} = 1 + \frac{\partial \beta_h}{\partial h} |_{h=h_*}$ , and it is

$$\Delta_{\hat{\phi}} = 1 + \frac{1 + \kappa}{2} \hat{\varepsilon} - \frac{1}{8} \left( 3 + \kappa \left( 3(\kappa + 2) + \frac{16\kappa^2(N + 2)}{(1 + 3\kappa)(N + 8)^2} \right) \right) \hat{\varepsilon}^2 + \mathcal{O}(\hat{\varepsilon}^3). \quad (4.15)$$

It is important to notice that the limit  $\kappa \rightarrow 0$  should not be considered, since there is no defect fixed point in that direction. The limit  $\kappa \rightarrow 1$ , instead, perfectly reproduces the existing results [46].

**One-point function.** The next piece of defect CFT data we consider is the one-point function of the bulk field  $\phi_1$ , which is the observable we used to renormalize the defect coupling. Defining

$$\langle \phi_a(x) \rangle = \delta_{a,1} \frac{\mathcal{N}_\phi a_\phi}{|x_\perp|^{\Delta_\phi}}, \quad (4.16)$$

and inserting the renormalized coupling in the diagrams in appendix A, we find

$$a_\phi^2 = \frac{(\kappa + 1)(N + 8)}{8\kappa} + \left( \frac{-15\kappa^2 - 18\kappa - 5}{4(3\kappa + 1)} + \frac{3(9\kappa^2 + 10\kappa + 3)}{2(3\kappa + 1)(N + 8)} + \frac{(3\kappa - 1)(\kappa + 1)(N + 8)}{32\kappa} + \frac{(\kappa + 1)^2(N + 8) \log(2)}{16\kappa} \right) \hat{\varepsilon} + \mathcal{O}(\hat{\varepsilon}^2). \quad (4.17)$$

When  $\kappa \rightarrow 1$ , we recover the result of [46].

**g-function.** Another important defect observable is the  $g$ -function of this DCFT, which obeys a monotonicity theorem under RG flow [76]. The computation is analogous to the one in [46], with the important difference that we keep a generic value of  $\Delta_\phi$  leading to a dependence on  $\kappa$ . For a free bulk theory, we can compute the defect expectation value of the circular defect exactly either by finding the classical solution to the equation of motion and computing the classical action or by resumming diagrams. The final result is

$$\log g_{\text{free}} = \log \frac{Z_{\text{defect}}}{Z_0} = \frac{2^{1-d} \pi^{\frac{3-d}{2}} \Gamma(\frac{1}{2} - \Delta_\phi) \Gamma(\Delta_\phi) R^{2-2\Delta_\phi}}{\Gamma(1 - \Delta_\phi) \Gamma(\frac{d}{2} - \Delta_\phi)}, \quad (4.18)$$

where  $R$  is the radius of the circle. Adding the bulk interaction, we have two diagrams up to order  $\hat{\varepsilon}$ , which were solved in [46] and we review in appendix C. The final result is

$$\log g = -\frac{(1 + \kappa) \hat{\varepsilon}}{16} h^2 + \frac{\kappa h^4 \lambda_*}{192 \pi^2 (3\kappa + 1)} + \mathcal{O}(\lambda_*^2), \quad (4.19)$$

and using the value of the defect fixed point coupling  $h_*$

$$\log g_{\text{IR}} = -\frac{(\kappa + 1)^3 (N + 8)}{32\kappa(3\kappa + 1)} \hat{\varepsilon} + \mathcal{O}(\hat{\varepsilon}^2) < 0 = \log g_{\text{UV}}, \quad (4.20)$$

as one expects from the  $g$ -theorem<sup>10</sup>.

<sup>10</sup> More precisely, the quantity that is monotonic under RG flow is the defect entropy, defined by  $s = (1 - R \frac{\partial}{\partial R}) \log g$ . However, as explained in [46],  $s$  and  $\log g$  agree at leading order.

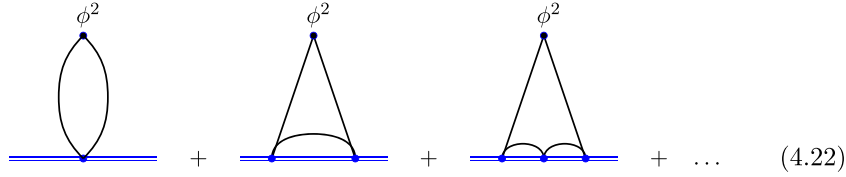
### 4.2. Surface defect

We now turn to another class of defects, which was analyzed in the short-range model in [54–56]. The surface defect is realized by integrating  $\phi^2$  over a two-dimensional plane<sup>11</sup>

$$S = S_0 + h_0 \int d^2\tau \phi_a \phi_a(\tau), \tag{4.21}$$

and, contrary to the localized magnetic field, it preserves the full  $O(N)$  symmetry.

To renormalize the defect coupling we consider the one-point function of  $\phi_a \phi^a$  (we need a  $O(N)$  singlet to get a non-vanishing one-point function). When the bulk is free, the  $\beta$  function can be computed exactly by going to momentum space and following the procedure described in [56] for resumming the diagrams



$$\tag{4.22}$$

This leads to the exact expression for the bare coupling


$$h_0 = \mu^{\frac{1+\kappa}{2}} \hat{\epsilon} h \left( 1 + \frac{2h}{(1+\kappa)\pi\hat{\epsilon}} + \left( \frac{2h}{(1+\kappa)\pi\hat{\epsilon}} \right)^2 + \dots \right) = \frac{\mu^{\frac{1+\kappa}{2}} \hat{\epsilon} h}{1 - \frac{2h}{(1+\kappa)\pi\hat{\epsilon}}}, \tag{4.23}$$

and consequently to the exact beta function

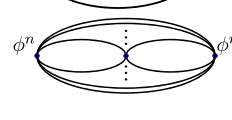
$$\beta_h = -\frac{1+\kappa}{2} \hat{\epsilon} h + \frac{h^2}{\pi}. \tag{4.24}$$

This admits a non-trivial fixed point in  $h_* = \frac{\pi(1+\kappa)}{2} \hat{\epsilon}$ .

Reintroducing the bulk coupling, we need to take into account the wavefunction renormalization of  $\phi^2$ , which will depend on the parameter  $\kappa$ . More generally, we can compute the renormalization of the field  $\phi^n$  for any positive integer  $n$ . This is given by the following bulk diagrams



$$= \frac{Nn! \left( \mathcal{N}_\phi^2 \right)^n}{|x|^{2n\Delta_\phi}}, \tag{4.25}$$



$$= -\frac{N(N+2)n!(n-1) \left( \mathcal{N}_\phi^2 \right)^{n+2} \lambda_0 \left( w_{4\Delta_\phi}^{(d)} \right)^2}{12} \frac{1}{w_{8\Delta_\phi-d}^{(d)} |x|^{(8+2n-4)\Delta_\phi-d}}. \tag{4.26}$$

The second diagram diverges, and we can introduce the wavefunction renormalization

$$Z_{\phi^n} = 1 - \frac{(N+2)n(n-1)}{6\kappa\hat{\epsilon}} \frac{\lambda}{(4\pi)^2} + \mathcal{O}(\lambda^2). \tag{4.27}$$

<sup>11</sup> There is also a symmetry-breaking version of this surface defect obtained by the interaction  $h^{ab} \phi_a \phi_b$ , with a generic tensor coupling  $h_{ab}$ . However, for simplicity we only consider the  $O(N)$  symmetric case.

The diagrams for the renormalization of the defect coupling  $h$  are given in appendix A. After taking into account the wavefunction renormalization  $Z_{\phi^2}$ , we find the following

$$\begin{aligned} h_0 &= \mu^{\frac{1+\kappa}{2}\hat{\varepsilon}} h \left( \frac{1}{1 - \frac{2h}{(1+\kappa)\pi\hat{\varepsilon}}} + \frac{(N+2)\lambda}{48\pi^2\kappa\hat{\varepsilon}} \right) + \mathcal{O}(h^2\lambda, h\lambda^2, \lambda^3), \\ \beta_h &= -\frac{1+\kappa}{2}\hat{\varepsilon}h + \frac{h^2}{\pi} + \frac{N+2}{48\pi^2}h\lambda. \end{aligned} \quad (4.28)$$

At  $\lambda = \lambda_*$ , we find a non-trivial defect fixed point

$$h_* = \frac{N(1-\kappa) + 8 + 4\kappa}{2(N+8)}\pi\hat{\varepsilon} + \mathcal{O}(\hat{\varepsilon}^2). \quad (4.29)$$

As expected, for  $\kappa = 1$  we recover the result of the short-range model [54–56]. In the opposite limit, and in contrast to the case of the localized magnetic field, there is no divergence at  $\kappa = 0$ . Instead, the fixed point gives  $h_* = \frac{\pi}{2}\hat{\varepsilon}$ , which is in agreement with the exact result found below for the Gaussian theory (4.24). Another notable difference from the localized magnetic field is that the fixed point is perturbatively small in  $\hat{\varepsilon}$ , rather than being of order  $\varepsilon^0$ .

Also in this case we can compute some interesting defect observables.

**Scaling dimension.** As before, a derivative of the beta function for  $h$  gives us access to the following defect scaling dimension at the fixed point:

$$\Delta_{\phi^2} = 2 + \frac{8 + 4\kappa + N(1-\kappa)}{2(N+8)}\hat{\varepsilon} + \mathcal{O}(\hat{\varepsilon}^2), \quad (4.30)$$

Once more, both limits  $\kappa = 1$  and  $\kappa = 0$  are well defined and they return the expected results for the short range and the Gaussian theory.

**One point data.** The Feynman diagrams we used to renormalize the coupling also give us access to the one-point function  $\langle\phi^2\rangle$

$$a_{\phi^2} = -\frac{\sqrt{N}(4\kappa + N(1-\kappa) + 8)}{4\sqrt{2}(N+8)}\hat{\varepsilon} + \mathcal{O}(\hat{\varepsilon}^2), \quad (4.31)$$

**Defect free energy.** The last observable we discuss is the defect free energy  $\mathcal{F}$ , which, in the case of surface defects, is a divergent quantity that contains a universal logarithmic term related to the Weyl anomaly coefficient. Specifically, for a two-dimensional defect, the Weyl anomaly takes the form

$$T_{\mu}^{\mu} \Big|_{\text{defect}} = -\frac{1}{24\pi} (b\mathcal{R}_{\Sigma} + d_1 K_{ab}^{\mu} K_{\mu}^{ab} - d_2 W_{ab}^{ab}), \quad (4.32)$$

where  $\mathcal{R}_{\Sigma}$  is the 2d Euler density,  $K_{ab}^{\mu}$  is the traceless extrinsic curvature, and  $W_{ab}^{ab}$  is the trace of the induced Weyl tensor on the surface  $\Sigma$ . The coefficient  $b$  satisfies a monotonicity theorem [77] and is determined by the logarithmic divergence of the defect free energy via the relation

$$\mathcal{F}_{\text{univ}} = -\frac{b}{3} \log(\mu R), \quad (4.33)$$

where  $\mu$  is the renormalization scale and  $R$  is the radius of the sphere.

The computation follows the one in [56], but with generic  $\Delta_\phi$ . Summing up the three diagrams shown in appendix C gives the following logarithmic term in the free energy

$$\mathcal{F}_{\text{univ}} = \left( \frac{N(1+\kappa)\hat{\varepsilon}h^2}{16\pi^2} - \frac{Nh^3}{12\pi^3} - \frac{N(N+2)\lambda h^2}{384\pi^4} \right) \log(\mu R). \quad (4.34)$$

This expression is very similar to the local case [54–56] apart from the  $\kappa$  dependence in the first term. At the defect fixed point we can compute the Weyl anomaly coefficient  $b$  finding

$$b_{\text{IR}} = -\frac{(8+4\kappa+N(1-\kappa))^3}{64(N+8)^3}\hat{\varepsilon}^3 + \mathcal{O}(\hat{\varepsilon}^4) < b_{\text{UV}} = 0, \quad (4.35)$$

which is consistent with the defect  $b$ -theorem [77].

## 5. Semiclassical construction of defects

In the previous sections, defects for the long-range  $O(N)$  model have been realized as fixed points of defect RG flows triggered by interactions that are classically marginal. However, strongly relevant interactions might as well originate a defect RG flow that ends in an IR fixed point. The latter case is in general more difficult to study, since the defect coupling is usually not perturbatively small. One way to get around this problem is to look for non-trivial saddle points of the path integral that respects the defect-conformal symmetry group. Perturbation theory around these new saddles can then be used to compute quantum corrections for various observables.

### 5.1. A warm-up example

Let us illustrate this idea with a simple example. Consider the local  $O(N)$  model, whose action is

$$S_{\text{bulk}} = \int d^d x \left( \frac{1}{2} (\partial\phi_a)^2 + \frac{\lambda_0}{4!} (\phi_a)^2 \right). \quad (5.1)$$

We can add an interaction localized on a  $p$ -dimensional defect

$$S_D = h_0 \int d^p \tau \phi_1. \quad (5.2)$$

When  $d = 4 - \hat{\varepsilon}$  and  $p = 1$ , the interaction is marginally relevant and one can therefore use standard diagrammatic techniques to compute observables [46, 70]. In the more general case, the beta function for the defect coupling reads

$$\beta_h = -(p - \Delta_\phi)h + \mathcal{O}(\lambda), \quad (5.3)$$

with  $\Delta_\phi = (d - 2)/2$ . If  $d = 4 - \hat{\varepsilon}$  (but with  $p$  generic), the bulk coupling constant undergoes a ‘short’ RG flow from the Gaussian fixed point to the Wilson–Fisher fixed point. At any scale  $\mu$  the following inequality holds

$$0 \leq \lambda(\mu) \leq \lambda_* = \frac{48\pi^2}{N+8}\hat{\varepsilon} + \mathcal{O}(\hat{\varepsilon}^2), \quad (5.4)$$

and in the IR limit we have  $\lim_{\mu \rightarrow 0} \lambda(\mu) = \lambda_*$ . Using this bound, we can solve (5.3) for  $h(\mu)$

$$h(\mu) = h(\mu_0) \left( \frac{\mu}{\mu_0} \right)^{-(p-\Delta_\phi)+\mathcal{O}(\hat{\varepsilon})}. \quad (5.5)$$

It is now evident that if  $p - \Delta_\phi \gg \hat{\varepsilon}$ , then  $h(\mu)$  rapidly flows to infinity in the IR limit, while  $\lambda(\mu)$  is still perturbatively small. This new phase of the theory should correspond to a non-trivial saddle point of the path integral. The saddle point is described by a classical profile  $\phi_{\text{cl}}^a(x)$  that satisfies the classical equations of motion. We can formulate an ansatz that respects all the symmetries of the problem

$$\phi_{\text{cl}}^a(x) = \delta_{a1} \frac{\mathcal{N}_\phi a_{\text{cl}}}{|x_\perp|^{\Delta_{\text{cl}}}}. \quad (5.6)$$

The equations of motion yield

$$\square \phi_{\text{cl}}^a(x) = \frac{\mathcal{N}_\phi a_{\text{cl}}}{|x_\perp|^{\Delta_{\text{cl}}+2}} (\Delta_{\text{cl}} (\Delta_{\text{cl}} + p + \varepsilon - 2)) \delta_{a1} = \frac{\lambda_0 \mathcal{N}_\phi^3 a_{\text{cl}}^3}{3! |x_\perp|^{3\Delta_{\text{cl}}}} \delta_{a1}. \quad (5.7)$$

This is readily solved

$$\Delta_{\text{cl}} = 1, \quad \mathcal{N}_\phi^2 a_{\text{cl}}^2 = \frac{6}{\lambda_0} (p + \hat{\varepsilon} - 1). \quad (5.8)$$

The two solutions for  $a_{\text{cl}}$  are associated to the  $\mathbb{Z}_2$  symmetry  $\phi_a \rightarrow -\phi_a$ , which is explicitly broken by the defect. In the following, we focus on the solution  $a_{\text{cl}} > 0$ . To compute observables, one can expand the bulk action around this new saddle point

$$\phi^a(x) = \phi_{\text{cl}}^a(x) + \delta\phi^a(x), \quad S'[\delta\phi^a] = \mathcal{S}_{\text{bulk}}[\phi_{\text{cl}}^a + \delta\phi^a] - \mathcal{S}_{\text{bulk}}[\phi_{\text{cl}}^a], \quad (5.9)$$

and then use standard diagrammatic techniques with the new action  $S'[\delta\phi^a]$ .<sup>12</sup> Note that  $\phi_{\text{cl}}^a(x)$  plays the role of a classical external source in this new action.

For some simple observables, the semiclassical analysis is sufficient to determine their value at the IR fixed point at leading order. For instance, for the order parameter we have

$$\langle \phi^a(x) \rangle = \phi_{\text{cl}}^a(x) + \langle \delta\phi^a(x) \rangle, \quad (5.10)$$

where the second term at the IR fixed point is of order  $\hat{\varepsilon}^{\frac{1}{2}}$  and is therefore subleading. Moreover, conformal symmetry imposes

$$\langle \phi^a(x) \rangle = \delta_{a1} \frac{\mathcal{N}_\phi a_\phi}{|x_\perp|^{\Delta_\phi}}. \quad (5.11)$$

From this it follows that at the IR fixed point

$$a_\phi^2 = a_{\text{cl}}^2 (1 + \mathcal{O}(\hat{\varepsilon})) = \frac{24\pi^2}{\lambda_*} (p - 1) + \mathcal{O}(\hat{\varepsilon}^0). \quad (5.12)$$

<sup>12</sup> In this realization, the presence of the defect is imposed through the ansatz (5.6) instead of an explicit defect term in the action.

For the boundary case  $p = 3 - \hat{\varepsilon}$ , this is indeed the correct value of the coefficient of the one-point function [73].

Note that for  $p = 1$  the leading-order contribution is vanishing as expected, since in that case the defect interaction is classically marginal. Interestingly, the equations of motion together with conformal symmetry can still be used to find the coefficient of the one-point function at leading order. Indeed, from the original action  $S$  it is evident that  $\langle \phi^a \phi^b \phi^b \rangle = \langle \phi^a \rangle \langle \phi^b \rangle \langle \phi^b \rangle + O(\lambda)$ . Assuming the form of the one-point function at the fixed point (5.11), the expectation value of the equation of motion then gives<sup>13</sup>

$$a_\phi^2 = \frac{N+8}{4} + O(\hat{\varepsilon}), \tag{5.13}$$

which agrees with the results of [46, 70] computed with Feynman diagrams.

### 5.2. The long-range $O(N)$ model

Now let us consider the long-range  $O(N)$  model with a localized magnetic field on a line. Recall that the action is

$$S = \int d^d x \left( \frac{1}{2} \phi_a \mathcal{L}_\sigma \phi_a + \frac{\lambda_0}{4!} (\phi_a)^2 \right) + h_0 \int d\tau \phi_1. \tag{5.14}$$

With  $\sigma = (d + \varepsilon)/2$ , the bulk interaction is weakly relevant. However, in this case  $\Delta_\phi = (d - \varepsilon)/4$ , and the defect interaction is strongly relevant for  $2 < d < 4$ . Therefore, standard perturbation theory around the trivial vacuum fails. Instead, we need to carry out an analysis similar to the one of last section.

**5.2.1. Semiclassics.** The first step to study this model is to look for non-trivial saddle points of the path integral of the form

$$\phi_{cl}^a(x) = \delta_{a1} \frac{\mathcal{N}_\phi a_{cl}}{|x_\perp|^{\Delta_{cl}}}. \tag{5.15}$$

The non-local equations of motion are

$$-\mathcal{L}_\sigma \phi_{cl}^a(x) = -\frac{2^{\frac{d+\varepsilon}{2}} \Gamma\left(\frac{d-1-\Delta_{cl}}{2}\right) \Gamma\left(\frac{d+\varepsilon+2\Delta_{cl}}{4}\right) \mathcal{N}_\phi a_{cl}}{\Gamma\left(\frac{\Delta_{cl}}{2}\right) \Gamma\left(\frac{d-2-\varepsilon-2\Delta_{cl}}{4}\right) |x_\perp|^{\Delta_{cl}+\frac{d+\varepsilon}{2}}} \delta_{a1} = \frac{\lambda_0 \mathcal{N}_\phi^3 a_{cl}^3}{3! |x_\perp|^{3\Delta_{cl}}} \delta_{a1}, \tag{5.16}$$

and they are solved by

$$\Delta_{cl} = \frac{d+\varepsilon}{4}, \quad \mathcal{N}_\phi^2 a_{cl}^2 = -\frac{6}{\lambda_0} \frac{2^{\frac{d+\varepsilon}{2}} \Gamma\left(\frac{3d-4-\varepsilon}{8}\right) \Gamma\left(\frac{3d+3\varepsilon}{8}\right)}{\Gamma\left(\frac{d-4-3\varepsilon}{8}\right) \Gamma\left(\frac{d+\varepsilon}{8}\right)}, \tag{5.17}$$

whereas before we select the solution  $a_{cl} > 0$ . Reasoning as in the previous section, we can conclude that

$$\langle \phi^a(x) \rangle = \delta_{a,1} \frac{\mathcal{N}_\phi a_\phi}{|x_\perp|^{\Delta_\phi}}. \tag{5.18}$$

<sup>13</sup> Note that this is not equivalent as taking  $p = 1$  in (5.8) and expanding. Indeed to get the correct result one need  $\Delta_\phi$  instead of  $\Delta_{cl}$ , together with the fact that at order  $O(\varepsilon)$  the operator  $\phi$  has no anomalous dimension.

with

$$\Delta_\phi = \frac{d-\varepsilon}{4}, \quad a_\phi^2 = a_{\text{cl}}^2 (1 + \mathcal{O}(\varepsilon)) = -\frac{(N+8)\Gamma(\frac{3d-4}{4})}{2^{\frac{d}{2}-1}\Gamma(\frac{d-4}{4})\Gamma(\frac{d}{2})\varepsilon} + \mathcal{O}(\varepsilon^0). \quad (5.19)$$

Note that for  $d = 4 + \mathcal{O}(\varepsilon)$  the leading-order contribution vanishes, since we get perturbatively close to the trivial vacuum. As in the previous example, by considering the expectation value of the equation of motion, we can compute the  $\mathcal{O}(\hat{\varepsilon})$  contribution to the coefficient  $a_\phi$  near  $d = 4$ , where the defect becomes weakly coupled. This result can then be matched to the results of section 4.1.

Let us briefly explain how the matching procedure works. In this section, we parameterize the defect conformal manifold (shown in figure 1) using the coordinates  $(d, \varepsilon)$ , near the crossover with GFF. In contrast, in section 4, we use the coordinates  $(\hat{\varepsilon}, k)$  near the point  $d = 4$ . To switch between these coordinate systems, we need to ensure that we are describing the same point  $(d, \sigma)$ . The corresponding condition is  $d = 4 - \hat{\varepsilon}$  and  $\varepsilon = \hat{\varepsilon}/k + \mathcal{O}(\hat{\varepsilon}^2)$ .

By considering the expectation value of the equation of motion and switching to the  $(\hat{\varepsilon}, k)$  coordinates, we obtain:

$$a_\phi^2 = \frac{(N+8)(\kappa+1)}{8\kappa} + \mathcal{O}(\hat{\varepsilon}), \quad (5.20)$$

which precisely matches the results in (4.16) and (4.17).

**5.2.2. Quantum corrections.** In order to compute quantum fluctuations around the new saddle point, we need to expand the action around it

$$S'[\delta\phi^a] = S_{\text{bulk}}[\phi_{\text{cl}}^a + \delta\phi^a] - S_{\text{bulk}}[\phi_{\text{cl}}^a] = \int d^d x \frac{1}{2} \left( (\delta^{ab} \mathcal{L}_\sigma + \frac{\lambda_0 \bar{\phi}^2}{6|x_\perp|^2 \Delta_{\text{cl}}} (\delta^{ab} + 2\delta^{a1} \delta^{b1})) \delta\phi_a \delta\phi_b + \frac{\lambda_0 \bar{\phi}}{6|x_\perp| \Delta_{\text{cl}}} \delta\phi_a \delta\phi_a \delta\phi_1 + \frac{\lambda_0}{4!} (\delta\phi_a)^2 \right). \quad (5.21)$$

For convenience, we have defined  $\bar{\phi} = \mathcal{N}_\phi a_{\text{cl}}$ . A similar analysis can also be done for a  $O(N)$  breaking surface defect [56]. In (5.21), there are new quadratic and cubic terms that break both Poincaré symmetry and  $O(N)$  symmetry to  $O(N-1)$ , as expected. The quadratic term comes with coefficient  $\lambda_0 \bar{\phi}^2$ , which, by (5.17), is a pure number. One can either try to invert the quadratic part of the action or treat this new term as a perturbation. In the latter case, since the coefficient is not small, one must always consider an arbitrary number of insertions of this term. This is what we will do in the following, since the inversion of the quadratic operator turns out to be a very difficult task. On the other hand, since  $\lambda_0 \bar{\phi} \sim \sqrt{\lambda_0}$ , the cubic term is perturbatively small.

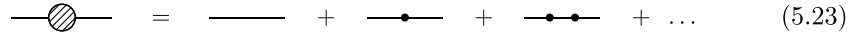
As an instructive example, we will set up the computation of the leading-order quantum corrections to the order parameter  $\langle \delta\phi_a(x) \rangle$ . For concreteness, we focus on the case  $d = 3$ , which is the physically relevant one. The following analysis is similar to the one carried out for the extraordinary surface transition in [73]. However, our case is more complicated due to

the fact that we have a line defect instead of a boundary. The diagrams contributing to this one-point function at order  $\sqrt{\lambda_0}$  all belong to a single family, which we can represent as follows



$$\delta\phi_a \text{ --- } \text{shaded circle} \text{ --- } \text{loop with two dots} \tag{5.22}$$

where the dots represent the quadratic and cubic interactions, and the ‘bubble’ is the dressed propagator defined by



$$\text{shaded circle} = \text{line} + \text{line with dot} + \text{line with two dots} + \dots \tag{5.23}$$

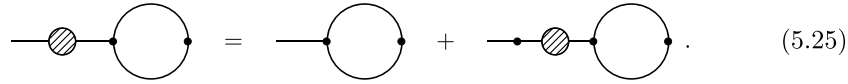
In (5.22) there is always at least one quadratic interaction inserted in the loop to avoid tadpole contributions. This diagram is already difficult to compute analytically, mainly because the terms in (5.23) involve challenging integrals, whose results must then be resummed.

We begin by extracting the divergent part of (5.22). It turns out that the divergence arises only from the following diagram



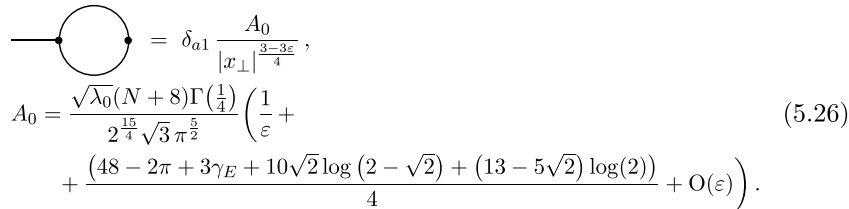
$$\delta\phi_a \text{ --- } \text{shaded circle} \text{ --- } \text{loop} \tag{5.24}$$

This can be verified by checking all the other diagrams and observing that they do not exhibit logarithmic divergences. To evaluate (5.24), we use the following recursion relation



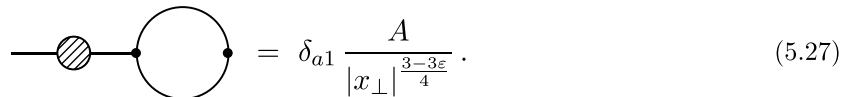
$$\text{shaded circle} \text{ --- } \text{loop} = \text{line} \text{ --- } \text{loop} + \text{line with dot} \text{ --- } \text{loop} \tag{5.25}$$

The first diagram on the right-hand side can be easily computed



$$\begin{aligned} \text{line} \text{ --- } \text{loop} &= \delta_{a1} \frac{A_0}{|x_\perp|^{\frac{3-3\epsilon}{4}}}, \\ A_0 &= \frac{\sqrt{\lambda_0}(N+8)\Gamma(\frac{1}{4})}{2^{\frac{15}{4}}\sqrt{3}\pi^{\frac{5}{2}}} \left( \frac{1}{\epsilon} + \right. \\ &\quad \left. + \frac{(48 - 2\pi + 3\gamma_E + 10\sqrt{2}\log(2 - \sqrt{2}) + (13 - 5\sqrt{2})\log(2))}{4} + O(\epsilon) \right). \end{aligned} \tag{5.26}$$

Using dimensional analysis, we can make the following ansatz for the left-hand side



$$\text{shaded circle} \text{ --- } \text{loop} = \delta_{a1} \frac{A}{|x_\perp|^{\frac{3-3\epsilon}{4}}}. \tag{5.27}$$

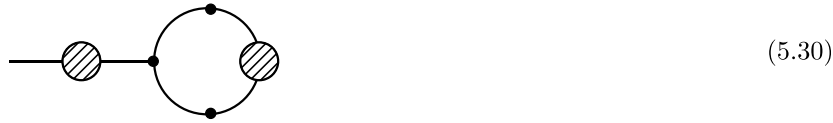
Substituting this ansatz into the recursion relation in (5.25), and evaluating the integral in the last term on the right-hand side, yields a linear equation that can be solved for  $A$

$$A = \frac{\sqrt{\lambda_0}(N+8)\Gamma(\frac{1}{4})}{2^{\frac{15}{4}}\sqrt{3}\pi^{\frac{5}{2}}} \left( \frac{1}{\epsilon} + + \frac{32 - 2\pi + 3\gamma_E + 13\log(2) - 3\sqrt{2}\log(2\sqrt{2} + 3)}{4} + O(\epsilon) \right). \tag{5.28}$$

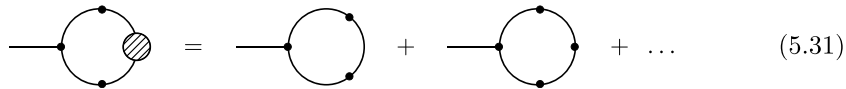
As we argued, (5.28) captures the full divergence of the more complicated diagram in (5.22). A non-trivial consistency check is that this divergence exactly cancels the one arising from the coupling renormalization in the classical term. More specifically, we have

$$\langle \phi_a(x) \rangle = \phi_{cl}^a + \langle \delta \phi_a(x) \rangle, \tag{5.29}$$

where  $\phi_{cl}^a \sim 1/\sqrt{\lambda_0}$  as given by (5.17). Since the bulk renormalizes independently, we also have that  $\lambda_0 = \mu^\epsilon \lambda(1 + \lambda(N+8)/(12\pi^2\epsilon) + \mathcal{O}(\lambda^2))$ , according to (2.11). Therefore, the first term in (5.22) has a divergence at order  $\sqrt{\lambda}$ , which is exactly canceled by the divergence in the second term that we just computed. This ensures that  $\langle \phi_a(x) \rangle$  remains finite. The finite term corresponds to the order  $\epsilon^0$  correction to (5.19). Part of this finite term is given in (5.28), while the rest comes from diagrams that contain more than one quadratic interaction in the loop. Their contributions can be collected into one single diagram



Furthermore, using a recursion similar to the one in (5.25), it suffices to compute the following



Unfortunately, performing this computation analytically is difficult. However, all the diagrams in the sum in (5.31) are finite for  $\epsilon = 0$  and can be evaluated numerically. The result of the sum can then be extrapolated using standard numerical techniques, such as Padé approximation. We leave this analysis for future investigations.

**Data availability statement**

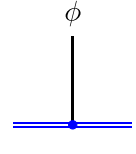
All data that support the findings of this study are included within the article (and any supplementary files).

**Acknowledgments**

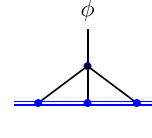
We would like to thank Adam Chalabi, Gabriel Cuomo, Charlotte Kristjansen, Marco Meineri, Edoardo Lauria and Miguel Paulos for useful discussions. EdS’s research is partially supported by the MUR PRIN contract 2020KR4KN2 ‘String Theory as a bridge between Gauge Theories and Quantum Gravity’ and by the INFN Project ST&FI ‘String Theory & Fundamental Interactions’.

### Appendix A. Diagrams for the defect coupling renormalization

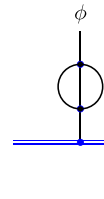
In this appendix, we list some of the diagrams that are relevant to the renormalization of defect couplings  $h$  in section 4. The first set of diagrams relates to the case of the localized magnetic field. Recall the notation  $w_A^{(d)} = (4\pi)^{d/2} 2^{-A} \Gamma(\frac{d-A}{2}) / \Gamma(\frac{A}{2})$



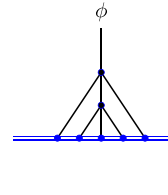
$$= -\mathcal{N}_\phi^2 h_0 \frac{\sqrt{\pi} \Gamma(\Delta_\phi - \frac{1}{2})}{\Gamma(\Delta_\phi)} \frac{1}{|x_\perp|^{2\Delta_\phi - 1}}, \quad (\text{A.1})$$



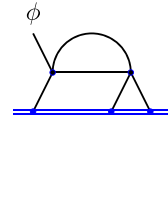
$$= \frac{(\mathcal{N}_\phi^2)^4 \lambda_0 h_0^3}{6} \left[ \frac{\sqrt{\pi} \Gamma(\Delta_\phi - \frac{1}{2})}{\Gamma(\Delta_\phi)} \right]^4 \frac{w_{2\Delta_\phi - 1}^{(d-1)} w_{6\Delta_\phi - 3}^{(d-1)}}{w_{8\Delta_\phi - 3 - d}^{(d-1)}} \frac{1}{|x_\perp|^{8\Delta_\phi - d - 3}}, \quad (\text{A.2})$$



$$= -\frac{(N+2)(\mathcal{N}_\phi^2)^5 \lambda_0^2 h_0}{18} \frac{\pi^{\frac{3}{2}} \Gamma(\Delta_\phi - \frac{1}{2})^2 \Gamma(3\Delta_\phi - \frac{1}{2})}{\Gamma(\Delta_\phi)^2 \Gamma(3\Delta_\phi)} \frac{w_{6\Delta_\phi - 1}^{(d-1)} [w_{2\Delta_\phi - 1}^{(d-1)}]^2}{w_{10\Delta_\phi - 2d - 1}^{(d-1)}} \frac{1}{|x_\perp|^{10\Delta_\phi - 2d - 1}}, \quad (\text{A.3})$$

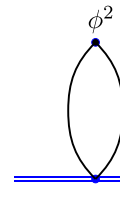


$$= -\frac{(\mathcal{N}_\phi^2)^7 \lambda_0^2 h_0^5}{12} \left[ \frac{\sqrt{\pi} \Gamma(\Delta_\phi - \frac{1}{2})}{\Gamma(\Delta_\phi)} \right]^7 \frac{[w_{2\Delta_\phi - 1}^{(d-1)}]^2 w_{6\Delta_\phi - 3}^{(d-1)} w_{12\Delta_\phi - d - 5}^{(d-1)}}{w_{8\Delta_\phi - d - 3}^{(d-1)} w_{14\Delta_\phi - 2d - 5}^{(d-1)}} \frac{1}{|x_\perp|^{14\Delta_\phi - 2d - 5}}, \quad (\text{A.4})$$

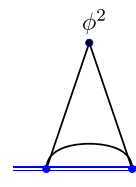


$$= -\frac{(N+8)(\mathcal{N}_\phi^2)^6 \lambda_0^2 h_0^3 \Gamma(\Delta_\phi - \frac{1}{2})^4 \pi^{\frac{5}{2}} \Gamma(2\Delta_\phi - \frac{1}{2})}{36 \Gamma(\Delta_\phi)^4 \Gamma(2\Delta_\phi)} \times \frac{w_{4\Delta_\phi - 1}^{(d-1)} w_{4\Delta_\phi - 2}^{(d-1)} w_{2\Delta_\phi - 1}^{(d-1)} w_{10\Delta_\phi - d - 3}^{(d-1)}}{w_{8\Delta_\phi - d - 2}^{(d-1)} w_{12\Delta_\phi - 2d - 3}^{(d-1)}} \frac{1}{|x_\perp|^{12\Delta_\phi - 2d - 3}}. \quad (\text{A.5})$$

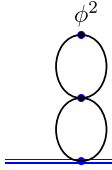
The second set of diagrams appears in the renormalization of the surface defect coupling



$$= -2h_0 (\mathcal{N}_\phi^2)^2 N \frac{\pi}{2\Delta_\phi - 1} \frac{1}{|x_\perp|^{4\Delta_\phi - 2}}, \quad (\text{A.6})$$



$$= 4 (\mathcal{N}_\phi^2)^3 N h_0^2 \frac{\pi^3 \Gamma(2\Delta_\phi - 1)^2 \Gamma(3\Delta_\phi - 2)}{\Gamma(\Delta_\phi)^3 \Gamma(4\Delta_\phi - 2) \sin(\pi\Delta_\phi)} \frac{1}{|x_\perp|^{6\Delta_\phi - 4}}, \quad (\text{A.7})$$



$$= \frac{h_0 \lambda_0 (N_\phi^2)^4 N(N+2)}{3} \frac{[w_{4\Delta_\phi}^{(d)}]^2}{w_{8\Delta_\phi-d}^{(d)}} \frac{\pi}{4\Delta_\phi-1-\frac{d}{2}} \frac{1}{|x_\perp|^{8\Delta_\phi-d-2}}. \tag{A.8}$$

**Appendix B. Useful integrals**

The diagrams above make use of the following integrals.

**Integral over a bulk vertex**

$$I(x) := \int \frac{d^d y}{|x-y|^A |y|^B} = \frac{w_A^{(d)} w_B^{(d)}}{w_{A+B-d}^{(d)}} \frac{1}{|x|^{A+B-d}} \tag{B.1}$$

**Integral over a defect vertex**

$$\int \frac{d^p \tau}{|x-x(\tau)|^\alpha} = \frac{\pi^{\frac{p}{2}} \Gamma(\frac{\alpha-p}{2})}{\Gamma(\frac{\alpha}{2})} \frac{1}{|x_\perp|^{\alpha-p}}. \tag{B.2}$$

**Integral over a bulk vertex with defect propagator**

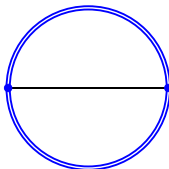
$$\int \frac{d^d y}{|x-y|^\alpha |y_\parallel|^\beta} = \frac{\pi^{\frac{d-p}{2}} \Gamma(\frac{\alpha-d+p}{2})}{\Gamma(\frac{\alpha}{2})} \frac{w_{\alpha-d+p}^{(p)} w_\beta^{(p)}}{w_{\alpha+\beta-d}^{(p)}} \frac{1}{|x_\parallel|^{\alpha+\beta-d}}. \tag{B.3}$$

**Three propagators.** The following integral is used in the renormalization of the surface defect coupling, and is particularly challenging to compute by hand (borrowing notation from [56], see [78] for a derivation). One way to proceed is to use Schwinger parametrization and the inversion formula for the gamma function

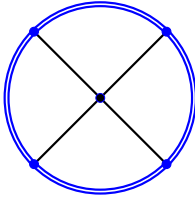
$$F = \int \frac{d^d k d^d l}{(k^2+m^2)^{\lambda_1} [(k+l)^2]^{\lambda_2} (l^2+m^2)^{\lambda_3}} = \frac{\pi^d \Gamma(\lambda_1+\lambda_2-\frac{d}{2}) \Gamma(\lambda_2+\lambda_3-\frac{d}{2}) \Gamma(\frac{d}{2}-\lambda_2) \Gamma(\lambda_1+\lambda_2+\lambda_3-d)}{\Gamma(\lambda_1) \Gamma(\lambda_3) \Gamma(\lambda_1+2\lambda_2+\lambda_3-d) \Gamma(\frac{d}{2})} \frac{1}{(m^2)^{\lambda_1+\lambda_2+\lambda_3-d}}. \tag{B.4}$$

**Appendix C. Diagrams for the g-function close to four dimensions**

First, we list the diagrams useful to the computation of the g-function close to four dimensions for the localized magnetic field. The second diagram is challenging to compute exactly, and the result up to  $\mathcal{O}(\hat{\varepsilon})$  given below makes use of the integral (C.9).

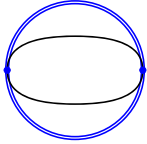


$$= \mathcal{N}_\phi^2 2^{1-2\Delta_\phi} h_0^2 R^{2-2\Delta_\phi} \pi \frac{\Gamma(\frac{1}{2}-\Delta_\phi) \sqrt{\pi}}{\Gamma(1-\Delta_\phi)}, \tag{C.1}$$

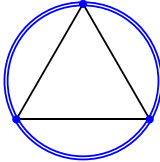


$$= -\frac{\lambda_0 h_0^4}{384\pi^2} + O(\hat{\varepsilon}). \tag{C.2}$$

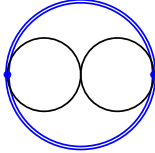
Second, the free energy for the surface defect is computed using the diagrams below



$$= h_0^2 (\mathcal{N}_\phi^2)^2 N \oint \frac{d^2 x d^2 y}{|x-y|^{4\Delta_\phi}} = -h_0^2 (\mathcal{N}_\phi^2)^2 N \frac{(2R)^{4(1-\Delta_\phi)} \pi^2}{2\Delta_\phi - 1}, \tag{C.3}$$



$$= -h_0^3 (\mathcal{N}_\phi^2)^3 \frac{4N}{3} R^{6(1-\Delta_\phi)} \frac{8\pi^{\frac{9}{2}} \Gamma(2-3\Delta_\phi)}{\Gamma(\frac{3}{2}-\Delta_\phi)^3}, \tag{C.4}$$



$$= -\lambda_0 h_0^2 (\mathcal{N}_\phi^2)^4 \frac{N(N+2)}{6} \frac{[w_{4\Delta_\phi}^{(d)}]^2}{w_{8\Delta_\phi-d}^{(d)}} \frac{(2R)^{d+4-8\Delta_\phi} \pi^2}{\frac{d}{2} + 1 - 4\Delta_\phi}. \tag{C.5}$$

*C.1. Useful integrals for the computation of g-functions*

The diagrams above make use of the following integrals.

**Circular integral over one angle**

$$\oint \frac{d\tau}{|x-x(\tau)|^{2\Delta}} = \int_{-\pi}^{\pi} \frac{R d\theta}{(|x_{\parallel}|^2 + |x_{\perp}|^2 + R^2 - 2R|x_{\parallel}|\cos\theta)^\Delta} \tag{C.6}$$

$$= \frac{2\pi R}{[ (|x_{\parallel}| + R)^2 + |x_{\perp}|^2 ]^\Delta} {}_2F_1\left(\frac{1}{2}, \Delta; 1, \frac{4R|x_{\parallel}|}{(|x_{\parallel}| + R)^2 + |x_{\perp}|^2}\right),$$

where we have used the integral representation of the hypergeometric function  ${}_2F_1$ .

**Circular integral over two angles**

$$\oint \frac{d\tau_1 d\tau_2}{|x(\tau_1) - x(\tau_2)|^{2\Delta}} = 4^{1-\Delta} R^{2-2\Delta} \pi \frac{\Gamma(\frac{1}{2} - \Delta) \sqrt{\pi}}{\Gamma(1 - \Delta)}. \tag{C.7}$$

**Second diagram in the g-function for the localized magnetic field.** The computation of diagram (C.2) is intricate. Calculating it amounts to evaluating the following quantity

$$-\frac{\lambda_0 h_0^4}{4!} (\mathcal{N}_\phi^2)^4 \int d^d x \left( \oint \frac{d\tau}{|x-x(\tau)|^{2\Delta_\phi}} \right)^4 = -\frac{\lambda_0 h_0^4}{4!} I. \tag{C.8}$$

The integral over the circular defect can be computed using equation (C.6). It simplifies to

$$I = 2\pi (2\pi R)^4 (\mathcal{N}_\phi^2)^4 S_{2-\varepsilon} \int_0^\infty dr \int_0^\infty dz \frac{r z^{3-\varepsilon}}{((r+R)^2+z^2)^{4-(1+\kappa)\varepsilon}} \left[ {}_2F_1\left(\frac{1}{2}, 1 - \frac{(1+\kappa)\varepsilon}{4}; 1, \frac{4rR}{(r+R)^2+z^2}\right) \right]^4. \quad (\text{C.9})$$

It is enough to give  $I$  to order  $\mathcal{O}(\varepsilon^0)$ , since  $\lambda_* \sim \hat{\varepsilon}$  and  $h_*$  is finite. The remaining integral can be conducted using appendix B in [46] and it evaluates to  $I = 1/(16\pi^2)$  in the limit  $\hat{\varepsilon} \rightarrow 0$ .

### Spherical integration over two angles

$$\oint \frac{d^2\tau_1 d^2\tau_2}{|x(\tau_1) - x(\tau_2)|^{2\Delta}} = \frac{(2R)^{4-2\Delta} \pi^2}{1 - \Delta}. \quad (\text{C.10})$$

### Appendix D. Integrating out $\hat{\psi}$

Let's study the effective theory for  $\phi$  when  $\hat{\psi}$  is integrated out in a theory described by the action (2.16). The effective action thus obtained yields results identical to those derived in the two-field picture, but it is nevertheless instructive to show that the relevant functional integrals can be conducted in some simple cases. Furthermore, having noticed that in  $d = 4$  the dimension  $\Delta_\psi \rightarrow 0$  for  $a = p$ , one might want to check whether or not the aforementioned action reduces to that of a localized magnetic field for  $a = p = 1$  (resp. surface defect for  $a = p = 2$ ) as  $d \rightarrow 4$ .

Throughout this section, we will be considering a free bulk, i.e.  $\lambda \rightarrow 0$ , and we will argue that in some cases where the defect GFF can be integrated out, there is no match with the localized magnetic field and the surface defect when  $d = 4 - \hat{\varepsilon}$ .

Let's set  $\sigma = d - 2\Delta_\phi$  and  $\tau = p - 2\Delta_\psi$ . To avoid conflicts and use lighter notation, we also drop the  $\tau$  parametrization of the defect and instead use  $y$  coordinates in this section only. It turns out that for  $b = 1$  or  $b = 2$ —which are the only cases we will look at—this integration can be carried out exactly. This amounts to the following rewriting of the partition function

$$Z = \int \mathcal{D}\phi e^{-S_0[\phi]} \int \mathcal{D}\psi e^{-S_1[\phi, \psi]} = \int \mathcal{D}\phi e^{-S_{\text{eff}}[\phi]}, \quad (\text{D.1})$$

where  $S_0[\phi]$  is the bulk action,  $S_1[\phi, \psi]$  is the defect action and the effective action is defined, up to a  $\phi$ -independent term, by

$$S_{\text{eff}}[\phi] := S_0[\phi] - \log \int \mathcal{D}\psi e^{-S_1[\phi, \psi]}. \quad (\text{D.2})$$

#### D.1. $b = 1$ theory

To integrate out  $\psi$  in the  $b = 1$  case, one can start by completing the square in the defect action

$$\begin{aligned} S_1[\phi, \psi] &= \frac{1}{2} \int_p [\psi \mathcal{L}_\tau \psi + g_0 \phi^a \psi] = \frac{1}{2} \int_p \left( \psi + \frac{g_0 \phi^a \mathcal{L}_{-\tau}}{4} \right) \mathcal{L}_\tau \left( \psi + \frac{g_0 \mathcal{L}_{-\tau} \phi^a}{4} \right) \\ &\quad - \frac{g_0^2}{16} \int_p \phi^a \mathcal{L}_{-\tau} \phi^a. \end{aligned} \quad (\text{D.3})$$

A simple translation of  $\psi$  makes the first term in  $S_1$   $\phi$ -independent, and the resulting path integral is a constant. We are hence left with

$$\begin{aligned} S_{\text{eff}}[\phi] &= \frac{1}{2} \int d^d x \phi \mathcal{L}_\sigma \phi - \frac{g_0^2}{16} \int d^p y \phi^a \mathcal{L}_{-\tau} \phi^a \\ &= \frac{1}{2} \int d^d x \phi \mathcal{L}_\sigma \phi - \frac{g_0^2}{16} \mathcal{N}_{-\tau} \int d^p y_1 d^p y_2 \frac{\phi^a(y_1) \phi^a(y_2)}{|y_1 - y_2|^{p-\tau}}. \end{aligned} \tag{D.4}$$

Taking  $d \rightarrow 4$  in the  $a = p$  case yields to lowest nontrivial order<sup>14</sup>

$$S_{\text{eff}}[\phi] = \frac{1}{2} \int d^d x \phi \mathcal{L}_\sigma \phi - \left( g_0 \int d^p y \phi^p(y) \right)^2, \tag{D.5}$$

since  $\Delta_\psi \rightarrow 0$ . This action clearly cannot be mapped to the localized magnetic field, nor to the surface defect by a simple redefinition of  $g_0$ .

### D.2. $b = 2$ theory

In the  $b = 2$  case, integrating out  $\psi$  amounts to evaluating a Gaussian integral,

$$S_1[\phi] = \frac{1}{2} \int dx \psi (\mathcal{L}_\tau + g_0 \phi^a) \psi. \tag{D.6}$$

This looks like a GFF,  $g\phi^a$  generating a mass-like term for  $\psi$ . We need to calculate the following functional integral to integrate this field out

$$\int \mathcal{D}\psi e^{-S_1} = C \det(\mathcal{L}_\tau + g_0 \phi^a)^{-1/2} = C e^{-\int d^d x \mathcal{L}_{\text{eff}}}, \tag{D.7}$$

where  $C$  is some normalization constant that is not important and we introduce an effective Lagrangian. Computing the effective action amounts to using the following identity for an operator  $\hat{A}$

$$\log \det \hat{A} = \text{Tr} \log \hat{A}. \tag{D.8}$$

Hence the difficult task of calculating a determinant can be recast into a trace calculation. The following equalities hold modulo a  $\phi$ -independent term

$$\begin{aligned} \text{Tr} \log(\mathcal{L}_\tau + g\phi^a) &= \int \frac{d^p k}{(2\pi)^p} \langle k | \log(\mathcal{L}_\tau + g_0 \phi^a) | k \rangle \\ &= \int \frac{d^p k}{(2\pi)^p} d^p x e^{ikx} \langle x | \log(\mathcal{L}_\tau + g_0 \phi^a) | k \rangle \\ &= \int \frac{d^p k}{(2\pi)^p} d^p x e^{ikx} \langle x | \log(1 + g_0 \mathcal{L}_\tau^{-1} \phi^a) | k \rangle \\ &= \sum_{j=1}^{+\infty} \frac{g_0^j (-1)^{j+1}}{j} \int d^p x \frac{d^p k}{(2\pi)^p} e^{ikx} \langle x | [\mathcal{L}_\tau^{-1} \phi^a]^j | k \rangle. \end{aligned} \tag{D.9}$$

<sup>14</sup> We ignore the normalization factor in front of  $g_0$ , since the coupling can be redefined to absorb it as we attempt to map to the localized magnetic field or the surface defect.

One can then use the following identity, easily derived using the action of the fractional Laplacian on plane waves,

$$\langle x | [\mathcal{L}_\tau^{-1} \phi^a]^j | k \rangle = e^{-ikx} \int \prod_{i=1}^j \frac{d^p q_i}{(2\pi)^p} \hat{\phi}^a(q_i) e^{iq_i x} \frac{1}{|q_1 + \dots + q_i - k|^\tau}. \quad (\text{D.10})$$

We finally get  $L_{\text{eff}} = \sum_j L_{\text{eff}}^{(j)}$  with

$$\begin{aligned} L_{\text{eff}}^{(j)} &= \frac{g_0^j (-1)^{j+1}}{2j} \int \frac{d^p k}{(2\pi)^p} \prod_{i=1}^j \frac{d^p q_i}{(2\pi)^p} \hat{\phi}^a(q_i) e^{iq_i x} \frac{1}{|q_1 + \dots + q_i - k|^\tau} \\ &= \frac{g_0^j (-1)^{j+1}}{2j} \phi(x)^a \int \frac{d^p k}{(2\pi)^p} \frac{1}{|k|^\tau} \prod_{i=2}^j \frac{d^p q_i}{(2\pi)^p} \hat{\phi}^a(q_i) e^{iq_i x} \frac{1}{|q_2 + \dots + q_i - k|^\tau} \\ &= \frac{g_0^j (-1)^{j+1}}{2j} \phi(x)^a \int \frac{d^p k}{(2\pi)^p} \frac{1}{|k|^\tau} \prod_{i=2}^j \frac{d^p q_i}{(2\pi)^p} d^p x_i \phi(x_i)^a e^{iq_i(x-x_i)} \frac{1}{|q_2 + \dots + q_i - k|^\tau}. \end{aligned} \quad (\text{D.11})$$

Reorganizing the complex exponentials allows one to rewrite this using known propagators, yielding

$$S_{\text{eff}} = \sum_{j=1}^{+\infty} \frac{(-1)^{j+1} (\mathcal{N}_\psi^2)^j}{2j} g_0^j \int \prod_{i=1}^j d^p x_i \frac{\phi(x_i)^a}{|x_{i+1} - x_i|^{p-\tau}}. \quad (\text{D.12})$$

Setting  $a = p = 1$  or  $2$  and taking  $d \rightarrow 4$ , the effective action becomes, to lowest nontrivial order

$$S_{\text{eff}}[\phi] = \frac{1}{2} \int d^d x \phi \mathcal{L}_\sigma \phi + \frac{1}{2} \log \left( 1 + g_0 \int d^p y \phi(y)^p \right). \quad (\text{D.13})$$

This action seems a lot closer to the localized magnetic field and the surface defect. As we have seen,  $g$  renormalizes in a few of the interesting cases, and the fixed point is infinitesimal. Hence, expanding the logarithm leads to

$$S_{\text{eff}} = \frac{1}{2} \int d^d x \phi \mathcal{L}_\sigma \phi + \frac{g_0}{2} \int d^p y \phi(y)^p + \dots \quad (\text{D.14})$$

Therefore, at the lowest orders, the theory does resemble the line or surface defects we studied. Notwithstanding, their behaviors diverge from one another as we include higher loop orders. One observable which exemplifies this is the  $g$ -function for the  $a = p = 1$  theory, which is readily accessible from the effective theory

$$g = \sum_{k=0}^{\infty} \frac{(4k)!}{(2k)!k!} \left[ g_0^2 2^{-3-2\Delta_\phi} \mathbf{R}^{2-2\Delta_\phi} \pi \frac{\Gamma(\frac{1}{2} - \Delta_\phi) \sqrt{\pi}}{\Gamma(1 - \Delta_\phi)} \right]^k. \quad (\text{D.15})$$

The above expression cannot directly be mapped to (4.18) by a redefinition of  $g_0$ . This is essentially because of the coefficients  $(4k)!/(2k)!k!$  making it depart from the series of an exponential. Incidentally, these coefficients also translate the different combinatorics in the two theories on the line. Indeed, when  $\Delta_\psi \rightarrow 0$ , some diagrams which were previously distinct become the same, and contribute non-trivially to the combinatorics.

## ORCID iDs

Lorenzo Bianchi  [0000-0001-6094-2559](https://orcid.org/0000-0001-6094-2559)

Leonardo S Cardinale  [0009-0006-8275-8350](https://orcid.org/0009-0006-8275-8350)

Elia de Sabbata  [0000-0003-2679-3646](https://orcid.org/0000-0003-2679-3646)

## References

- [1] Rychkov S and Su N 2024 New developments in the numerical conformal bootstrap *Rev. Mod. Phys.* **96** 045004
- [2] Fisher M E, Ma S-K and Nickel B G 1972 Critical exponents for long-range interactions *Phys. Rev. Lett.* **29** 917
- [3] Sak J 1977 Low-temperature renormalization group for ferromagnets with long-range interactions *Phys. Rev. B* **15** 4344
- [4] Sak J 1973 Recursion relations and fixed points for ferromagnets with long-range interactions *Phys. Rev. B* **8** 281
- [5] Aizenman M and Fernández R 1988 Critical exponents for long-range interactions *Lett. Math. Phys.* **16** 39
- [6] Honkonen J and Nalimov M Y 1989 Crossover between field theories with short-range and long-range exchange or correlations *J. Phys. A: Math. Gen.* **22** 751
- [7] Honkonen J 1990 Critical behaviour of the long-range ( $\phi^2$ )<sub>2</sub> model in the short-range limit *J. Phys. A: Math. Gen.* **23** 825
- [8] Picco M 2012 Critical behavior of the Ising model with long range interactions (arXiv:1207.1018)
- [9] Angelini M C, Parisi G and Ricci-Tersenghi F 2014 Relations between short-range and long-range Ising models *Phys. Rev. E* **89** 062120
- [10] Adelhardt P, Koziol J A, Schellenberger A and Schmidt K P 2020 Quantum criticality and excitations of a long-range anisotropic XY chain in a transverse field *Phys. Rev. B* **102** 174424
- [11] Luijten E and Blöte H W J 2002 Boundary between long-range and short-range critical behavior in systems with algebraic interactions *Phys. Rev. Lett.* **89** 025703
- [12] Zhao J, Song M, Qi Y, Rong J and Meng Z Y 2023 Finite-temperature critical behaviors in 2D long-range quantum Heisenberg model *npj Quantum Mater.* **8** 59
- [13] Paulos M F, Rychkov S, van Rees B C and Zan B 2016 Conformal invariance in the long-range Ising model *Nucl. Phys. B* **902** 246
- [14] Behan C, Rastelli L, Rychkov S and Zan B 2017 Long-range critical exponents near the short-range crossover *Phys. Rev. Lett.* **118** 241601
- [15] Behan C, Rastelli L, Rychkov S and Zan B 2017 A scaling theory for the long-range to short-range crossover and an infrared duality *J. Phys. A: Math. Theor.* **50** 354002
- [16] Benedetti D, Gurau R, Harribey S and Suzuki K 2020 Long-range multi-scalar models at three loops *J. Phys. A: Math. Theor.* **53** 445008
- [17] Benedetti D, Gurau R, Harribey S and Lettera D 2024 Finite-size versus finite-temperature effects in the critical long-range O(N) model *J. High Energy Phys.* **JHEP02(2024)078**
- [18] Benedetti D, Gurau R and Lettera D 2024 Dynamic critical exponent in quantum long-range models *Phys. Rev. B* **110** 104102
- [19] Behan C 2019 Bootstrapping the long-range Ising model in three dimensions *J. Phys. A: Math. Theor.* **52** 075401
- [20] Behan C, Lauria E, Nocchi M and van Vliet P 2024 Analytic and numerical bootstrap for the long-range Ising model *J. High Energy Phys.* **JHEP03(2024)136**
- [21] Chai N, Goykhman M and Sinha R 2021 Long-range vector models at large N *J. High Energy Phys.* **JHEP09(2021)194**
- [22] Chakraborty S and Goykhman M 2021 Critical long-range vector model in the UV *J. High Energy Phys.* **JHEP10(2021)151**
- [23] Giombi S, Helfenberger E and Khanchandani H 2023 Long range, large charge, large N *J. High Energy Phys.* **JHEP01(2023)166**
- [24] Chai N, Chakraborty S, Goykhman M and Sinha R 2022 Long-range fermions and critical dualities *J. High Energy Phys.* **JHEP01(2022)172**
- [25] Rong J 2024 Local/short-range conformal field theories from long-range perturbation theory (arXiv:2406.17958)

- [26] Li Z 2024 Conformality loss and short-range crossover in long-range conformal field theories (arXiv:2409.19392)
- [27] Billò M, Gonçalves V, Lauria E and Meineri M 2016 Defects in conformal field theory *J. High Energy Phys.* **JHEP04(2016)091**
- [28] Vojta M, Buragohain C and Sachdev S 2000 Quantum impurity dynamics in two-dimensional anti-ferromagnets and superconductors *Phys. Rev. B* **61** 15152
- [29] Sachdev S, Buragohain C and Vojta M 1999 Quantum impurity in a nearly critical two-dimensional antiferromagnet *Science* **286** 2479
- [30] Sachdev S 2001 Static hole in a critical antiferromagnet: field-theoretic renormalization group *Physica C* **357–360** 78
- [31] Sachdev S and Vojta M 2003 Quantum impurity in an antiferromagnet: nonlinear sigma model theory *Phys. Rev. B* **68** 064419
- [32] Billò M, Caselle M, Gaiotto D, Gliozzi F, Meineri M and Pellegrini R 2013 Line defects in the 3d Ising model *J. High Energy Phys.* **JHEP07(2013)055**
- [33] Deng Y J, Blote H W J and Nightingale M P 2005 Surface and bulk transitions in three-dimensional  $O(n)$  models *Phys. Rev. E* **72** 016128
- [34] Toldin F P 2021 Boundary critical behavior of the three-dimensional Heisenberg universality class *Phys. Rev. Lett.* **126** 135701
- [35] Metlitski M A 2022 Boundary criticality of the  $O(N)$  model in  $d = 3$  critically revisited *SciPost Phys.* **12** 131
- [36] Toldin F P and Metlitski M A 2022 Boundary criticality of the 3D  $O(N)$  model: from normal to extraordinary *Phys. Rev. Lett.* **128** 215701
- [37] Liendo P, Rastelli L and van Rees B C 2013 The bootstrap program for boundary  $CFT_d$  *J. High Energy Phys.* **JHEP07(2013)113**
- [38] Bissi A, Hansen T and Söderberg A 2019 Analytic bootstrap for boundary  $CFT$  *J. High Energy Phys.* **JHEP01(2019)010**
- [39] Padayasi J, Krishnan A, Metlitski M A, Gruzberg I A and Meineri M 2021 The extraordinary boundary transition in the 3d  $O(N)$  model via conformal bootstrap (arXiv:2111.03071)
- [40] Gimenez-Grau A, Lauria E, Liendo P and van Vliet P 2022 Bootstrapping line defects with  $O(2)$  global symmetry *J. High Energy Phys.* **JHEP11(2022)018**
- [41] Bianchi L, Bonomi D and de Sabbata E 2023 Analytic bootstrap for the localized magnetic field *J. High Energy Phys.* **JHEP04(2023)069**
- [42] Gimenez-Grau A 2022 Probing magnetic line defects with two-point functions (arXiv:2212.02520)
- [43] Bianchi L, Bonomi D, de Sabbata E and Gimenez-Grau A 2024 Analytic bootstrap for magnetic impurities *J. High Energy Phys.* **JHEP05(2024)080**
- [44] Belton J, Drukker N, Kong Z and Stergiou A 2025 Fine spectrum from crude analytic bootstrap (arXiv:2503.07710)
- [45] Liu S, Shapourian H, Vishwanath A and Metlitski M A 2021 Magnetic impurities at quantum critical points: large  $N$  expansion and connections to symmetry protected topological states *Phys. Rev. B* **104** 104201
- [46] Cuomo G, Komargodski Z and Mezei M 2022 Localized magnetic field in the  $O(N)$  model *J. High Energy Phys.* **JHEP02(2022)134**
- [47] Cuomo G, Komargodski Z, Mezei M and Raviv-Moshe A 2022 Spin impurities, Wilson lines and semiclassics *J. High Energy Phys.* **JHEP06(2022)112**
- [48] Rodriguez-Gomez D 2022 A scaling limit for line and surface defects *J. High Energy Phys.* **JHEP06(2022)071**
- [49] Rodriguez-Gomez D and Russo J G 2022 Defects in scalar field theories, RG flows and dimensional disentangling *J. High Energy Phys.* **JHEP11(2022)167**
- [50] Nishioka T, Okuyama Y and Shimamori S 2023 The epsilon expansion of the  $O(N)$  model with line defect from conformal field theory *J. High Energy Phys.* **JHEP03(2023)203**
- [51] Pannell W H and Stergiou A 2023 Line defect RG flows in the  $\epsilon$  expansion *J. High Energy Phys.* **JHEP06(2023)186**
- [52] Pannell W H 2024 A note on defect stability in  $d = 4 - \epsilon$  (arXiv:2408.15315)
- [53] Krishnan A and Metlitski M A 2023 A plane defect in the 3d  $O(N)$  model *SciPost Phys.* **15** 090
- [54] Trépanier M 2023 Surface defects in the  $O(N)$  model *J. High Energy Phys.* **JHEP09(2023)074**
- [55] Raviv-Moshe A and Zhong S 2023 Phases of surface defects in Scalar Field Theories *J. High Energy Phys.* **JHEP08(2023)143**

- [56] Giombi S and Liu B 2023 Notes on a surface defect in the  $O(N)$  model *J. High Energy Phys.* [JHEP12\(2023\)004](#)
- [57] Nishioka T, Okuyama Y and Shimamori S 2023 Comments on epsilon expansion of the  $O(N)$  model with boundary *J. High Energy Phys.* [JHEP03\(2023\)051](#)
- [58] Harribey S, Klebanov I R and Sun Z 2023 Boundaries and interfaces with localized cubic interactions in the  $O(N)$  model *J. High Energy Phys.* [JHEP10\(2023\)017](#)
- [59] Shachar T 2024 On intersecting conformal defects (arXiv:[2411.14543](#))
- [60] de Sabbata E, Drukker N and Stergiou A 2024 Transdimensional defects (arXiv:[2411.17809](#))
- [61] Giombi S and Khanchandani H 2020  $O(N)$  models with boundary interactions and their long range generalizations *J. High Energy Phys.* [JHEP08\(2020\)010](#)
- [62] Lauria E, Liendo P, Van Rees B C and Zhao X 2021 Line and surface defects for the free scalar field *J. High Energy Phys.* [JHEP01\(2021\)060](#)
- [63] Bianchi L, Chalabi A, Procházka V, Robinson B and Sisti J 2021 Monodromy defects in free field theories *J. High Energy Phys.* [JHEP08\(2021\)013](#)
- [64] Chalabi A, Herzog C P, Ray K, Robinson B, Sisti J and Stergiou A 2022 Boundaries in free higher derivative conformal field theories (arXiv:[2211.14335](#))
- [65] Di Pietro L, Lauria E and Niro P 2024 Conformal boundary conditions for a 4d scalar field *SciPost Phys.* **16** 090
- [66] Bashmakov V and Sisti J 2024 Exploring defects with degrees of freedom in free scalar CFTs (arXiv:[2410.01716](#))
- [67] Hernández-Cuenca S 2024 Wormholes and factorization in exact effective theory (arXiv:[2404.10035](#))
- [68] Behan C C 2019 Bootstrapping some continuous families of conformal field theories *PhD Thesis* Stony Brook University
- [69] Caffarelli L and Silvestre L 2007 An extension problem related to the fractional Laplacian *Commun. PDE* **32** 1245
- [70] Allais A and Sachdev S 2014 Spectral function of a localized fermion coupled to the Wilson-Fisher conformal field theory *Phys. Rev. B* **90** 035131
- [71] Ohno K and Okabe Y 1984 The  $1/n$  expansion for the extraordinary transition of semi-infinite system *Prog. Theor. Phys.* **72** 736
- [72] McAvity D M and Osborn H 1995 Conformal field theories near a boundary in general dimensions *Nucl. Phys. B* **455** 522
- [73] Shpot M A 2021 Boundary conformal field theory at the extraordinary transition: the layer susceptibility to  $O(\epsilon)$  *J. High Energy Phys.* [JHEP01\(2021\)055](#)
- [74] Buhl-Mortensen I, de Leeuw M, Ipsen A C, Kristjansen C and Wilhelm M 2017 A quantum check of AdS/dCFT *J. High Energy Phys.* [JHEP01\(2017\)098](#)
- [75] Kristjansen C and Zarembo K 2024 't Hooft loops in  $N = 4$  super-Yang-Mills (arXiv:[2412.01972](#))
- [76] Cuomo G, Komargodski Z and Raviv-Moshe A 2022 Renormalization group flows on line defects *Phys. Rev. Lett.* **128** 021603
- [77] Jensen K and O'Bannon A 2016 Constraint on defect and boundary renormalization group flows *Phys. Rev. Lett.* **116** 091601
- [78] Smirnov V A 2006 *Feynman Integral Calculus* (Springer)